Electronic Supplementary Information (ESI)

Structural elucidation of HIV-1 G-quadruplexes in cellular environment and their ligand binding using responsive ^{19}F-labeled nucleoside probes

Sarupa Roy,[a] Priyasha Majee,[b] Sruthi Sudhakar,[b] Satyajit Mishra,[c] Jeet Kalia,[c,d] P. I. Pradeepkumar[b*] and Seergazhi G. Srivatsan[a*]

[a]Department of Chemistry, Indian Institute of Science Education and Research (IISER), Pune Dr. Homi Bhabha Road, Pune 411008, India. E-mail: srivatsan@iiserpune.ac.in

[b]Department of Chemistry, Indian Institute of Technology Bombay, Mumbai 400076, India. E-mail: pradeep@chem.iitb.ac.in

[c]Department of Biological Sciences, Indian Institute of Science Education and Research (IISER) Bhopal, Bhopal Bypass Road, Bhauri, Bhopal 462066, India.

[d]Department of Chemistry, Indian Institute of Science Education and Research (IISER) Bhopal, Bhopal Bypass Road, Bhauri, Bhopal 462066, India.

1. Materials: 5-Flurobenzofuran-2'-deoxyuridine (**1**) and phosphoramidite substrates (**1a**) and (**2a**) were synthesised following a reported procedure.[S1-S3] 5-fluoro-2'-deoxyuridine (**2**) was purchased from Carbosynth. Monomers for solid-phase oligonucleotide (ON) synthesis such as *N*-benzoyl-protected dA, *N*-acetyl-protected dC, *N,N*-dimethylformamide-protected dG, and dT phosphoramidite substrates were purchased from ChemGenes, Glen Research and Innovassynth. Solid supports for DNA synthesis were procured from Glen Research. All other reagents needed for solid-phase ON synthesis were availed from Sigma-Aldrich. Control DNA ONs **3**, **7**, **8**, **11** and **12** were purchased from Integrated DNA Technology, purified by denaturing polyacrylamide gel electrophoresis (PAGE) and desalted using Sep-Pak Classic C18 cartridges (Waters Corporation). BRACO19 hydrochloride and all reagents (Bio-Ultra grade) used in the preparation of buffers were purchased from Sigma-Aldrich. TMPyP4 and Doxorubicin hydrochloride (DOX) were procured from Merck-Millipore. Millipore water after autoclaving was used for the preparation of all buffer solutions and in all biophysical studies.

2. Instruments: NMR spectra of small molecules were acquired in Bruker AVANCE III HD ASCEND 400 MHz spectrometer and processed using Mnova software from Mestrelab Research. Mass data was obtained using ESI-MS Waters Synapt G2-Si Mass Spectrometry instrument. Modified DNA ONs were synthesized on a K&A DNA/RNA synthesizer H6. RP-HPLC analysis was performed using Agilent Technologies 1260 Infinity HPLC. Absorption spectra were recorded on a UV-2600 Shimadzu spectrophotometer. Fluorescence of the ONs samples were recorded using a Fluoromax-4 spectrophotometer (Horiba Scientific). UV-thermal melting analysis of the ONs was carried out on Cary 300 Bio UV-Vis spectrophotometer and Cary 3500 multicell UV-Vis spectrophotometer. CD measurements were done on a JASCO J-815 CD spectrometer. NMR spectra of the ONs were acquired on a Bruker AVANCE III HD ASCEND 600 MHz spectrometer equipped with Cryo-Probe (CP2.1 QCl 600S3 H/F-C/N-D-05 Z XT) and processed using Bruker TopSpin Software.

3. Solid-phase DNA synthesis: FBFdU (**1**) and or FdU (**2**) modified DNA ONs **4**–**6**, **9**, **10** and **13**–**16** were synthesized on a 1 µmole scale (1000 Å CPG solid support) with K&A H-6 synthesizer using phosphoramidite substrates. For modified phosphoramidites FBFdU (**1a**) and FdU (**2a**), double coupling of 3 min each was set (total 6 min). After the synthesis, the ONs were cleaved from the solid support using 30% aqueous ammonia and deprotected at 65 °C for 20 h. ONs were purified by denaturing PAGE (18 % or 20% gel) and the product bands were visualized by UV-shadowing. Product bands were excised and ONs were extracted with 4 mL of 0.5 M ammonium acetate buffer in a poly-prep column (Bio-Rad) for 12 h. Desalting was performed using a Waters C-18 cartridge. The purity of ONs was monitored by RP-HPLC (Figure S1). The integrity was verified by ESI-MS (Figure S2).

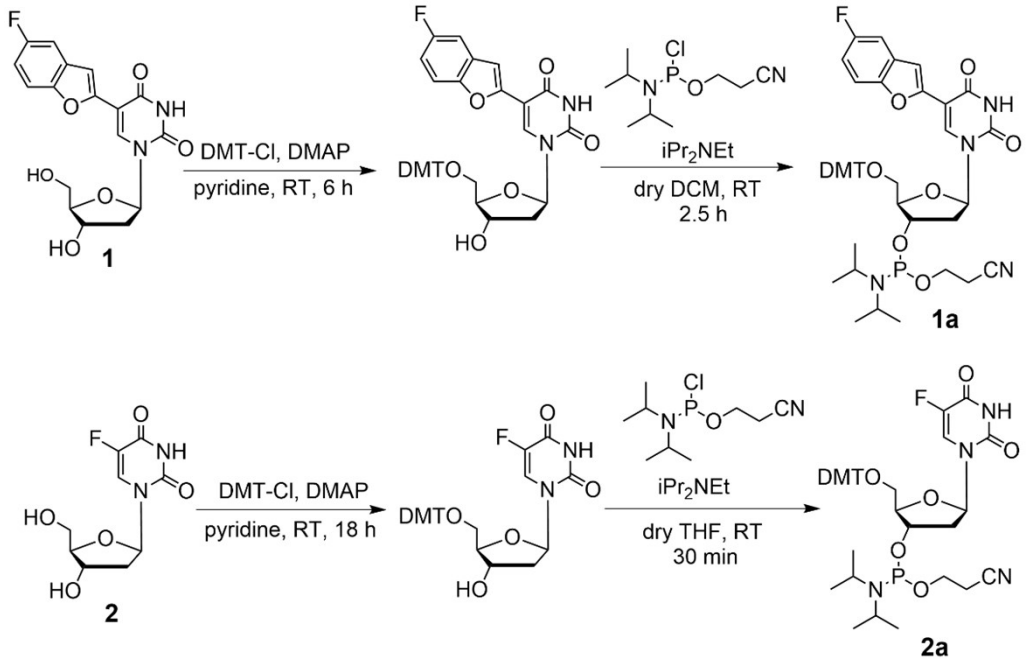

Scheme S1. FBFdU phosphoramidite (**1a**) and FdU phosphoramidite (**2a**) were synthesized following reported procedures.[S1-S3] ^{31}P NMR spectra of phosphoramidites (**1a**) and (**2a**) are enclosed at the end of the ESI.

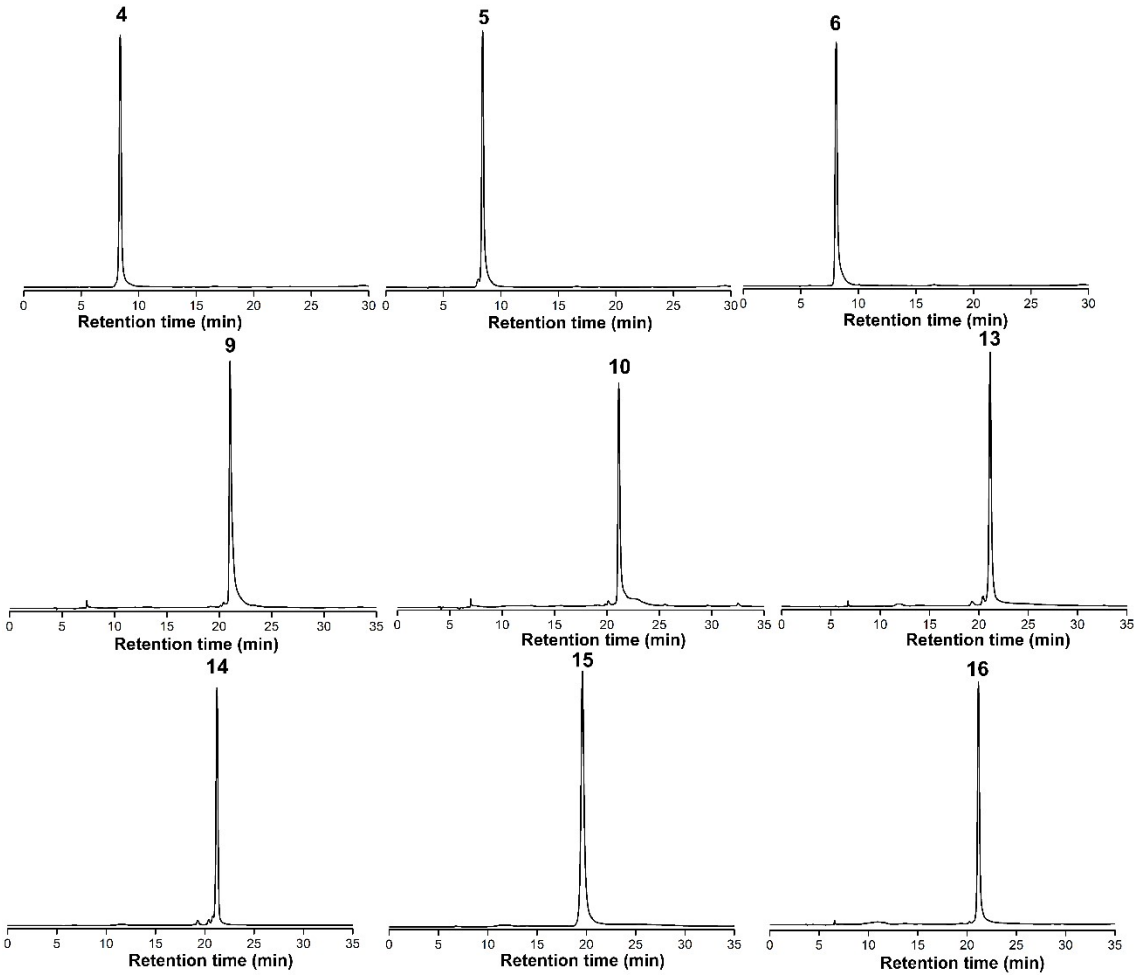

Fig. S1. The purity of PAGE purified ONs containing the modification was analysed by RP-HPLC at 260 nm using Luna C18 column (250 x 4.6 mm, 5 micron). Mobile phase A= 0.5 mM triethylammonium acetate (pH=7.3) and B= acetonitrile. Gradient: 0–100 % B in 30 min with a flow rate of 1 mL/min was used for ONs **4**–**6**. Gradient: 0–30 % B in 40 min and 30–100% in 10 min with a flow rate of 1 mL/min was used for ONs **9**, **10**, **13**–**16**.

4. ESI-MS analysis: Negative mode ESI-MS analysis was performed by injecting DNA ONs (~800 pmol) dissolved in 50% acetonitrile in an aqueous solution of 10 mM triethylamine and 100 mM 1,1,1,3,3,3-hexafluoro-2-propanol. See Figure S2 for mass spectra and Table S1 for details.

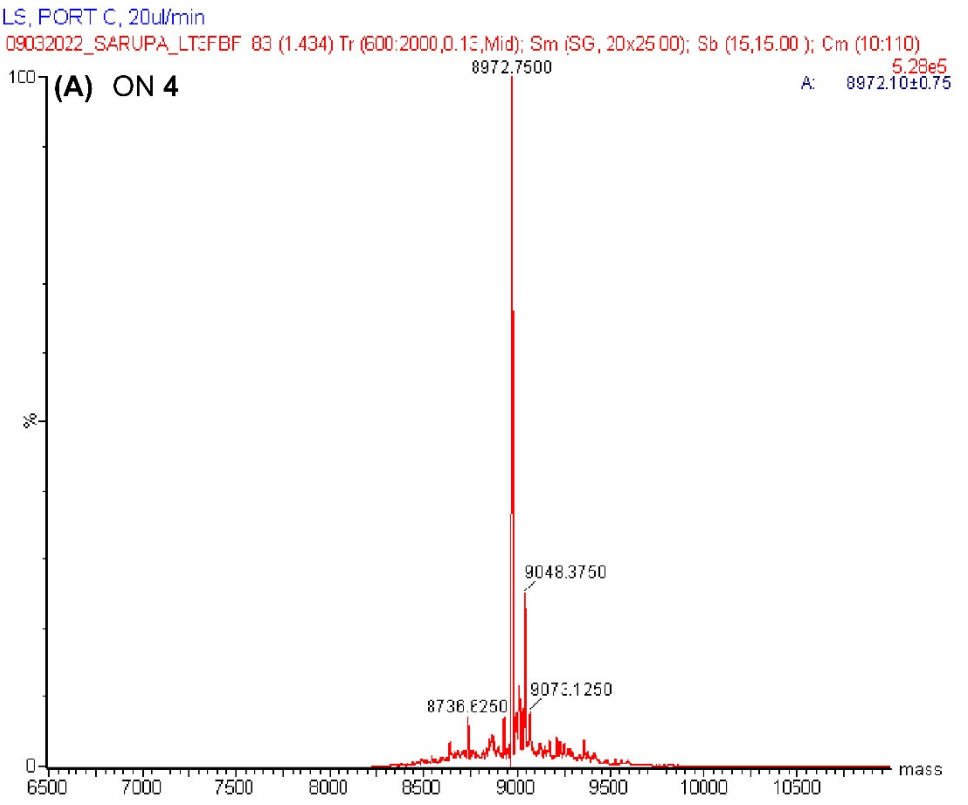
LS, PORT C, 20ul/min
09032022_SARUPA_LTEFBF 83 (1.434) Tr (600:2000,0.13,Mid); Sm (SG, 20x25.00); Sb (15,15.00); Cm (10:110)
(A) ON 4
8972.7500
5.28e5
A: 8972.10±0.75
9048.3750
8736.6250
100
%
0
6500
7000
7500
8000
8500
9000
9500
10000
10500
mass

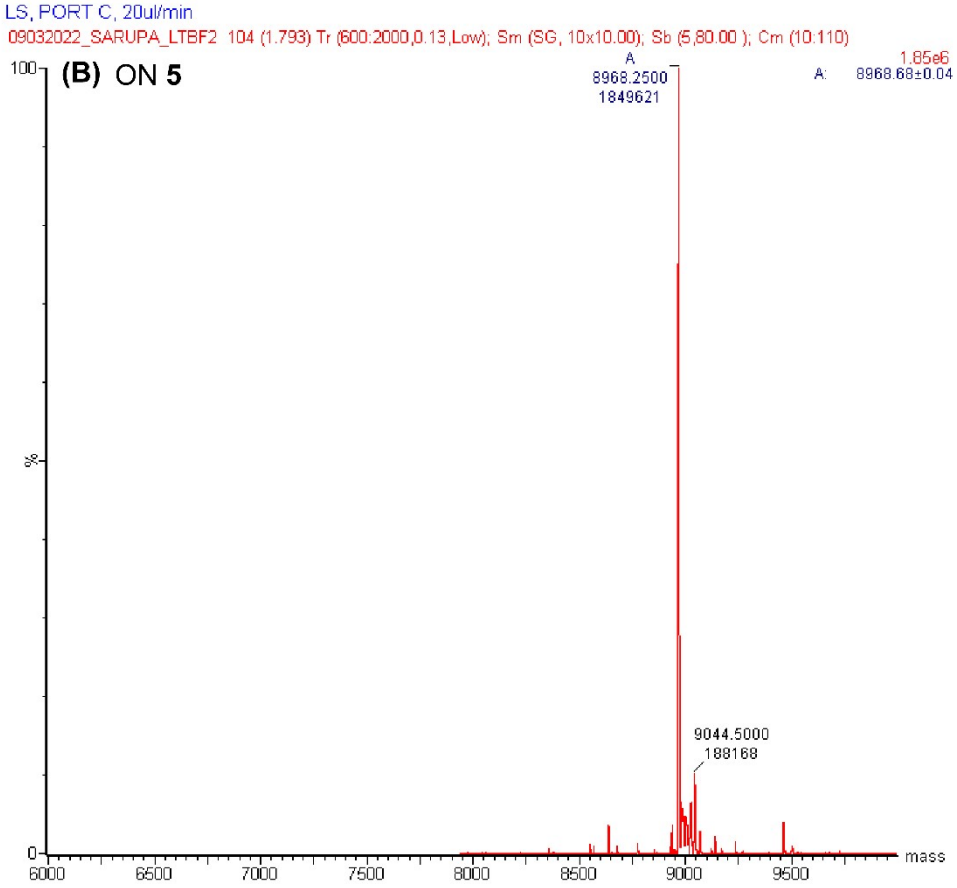
LS, PORT C, 20ul/min
09032022_SARUPA_LTBF2 104 (1.793) Tr (600:2000,0.13,Low); Sm (SG, 10x10.00); Sb (5,80.00); Cm (10:110)
(B) ON 5
A
8968.2500
1849621
1.85e6
A: 8968.68±0.04
9044.5000
188168
100
%
0
6000
6500
7000
7500
8000
8500
9000
9500
mass

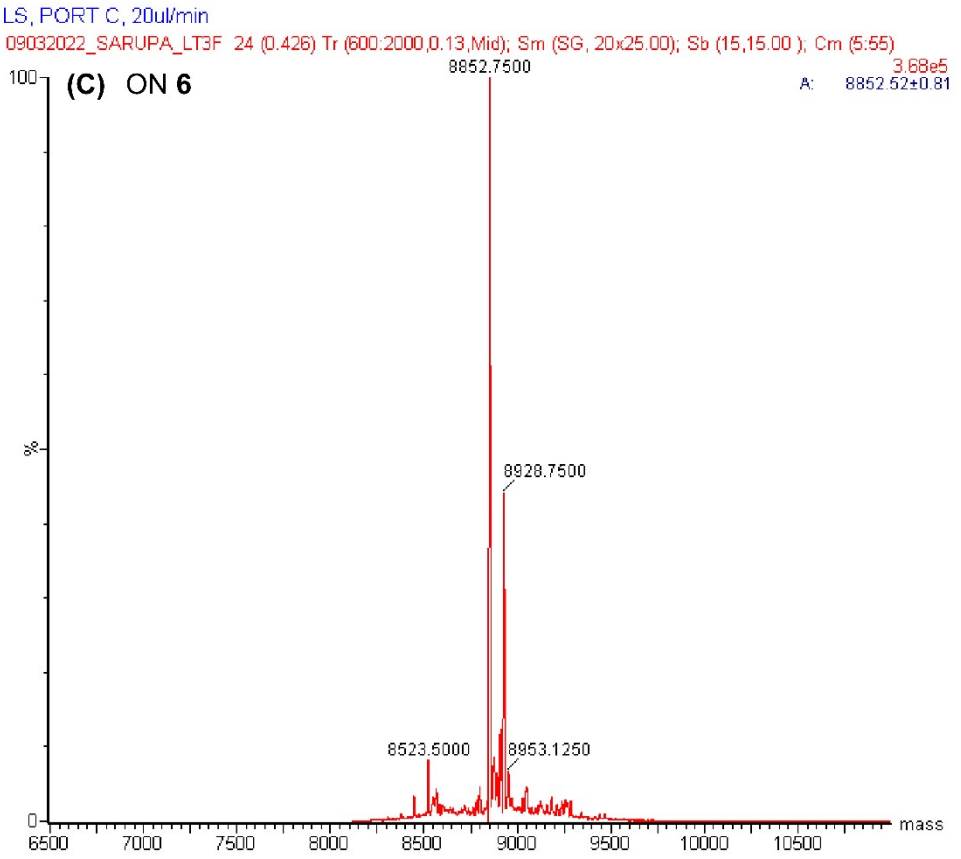
LS, PORT C, 20ul/min
09032022_SARUPA_LT3F 24 (0.426) Tr (600:2000,0.13,Mid); Sm (SG, 20x25.00); Sb (15,15.00); Cm (5:55)
(C) ON 6
3.68e5
A: 8852.52±0.81
8852.7500
8928.7500
8523.5000
8953.1250
mass

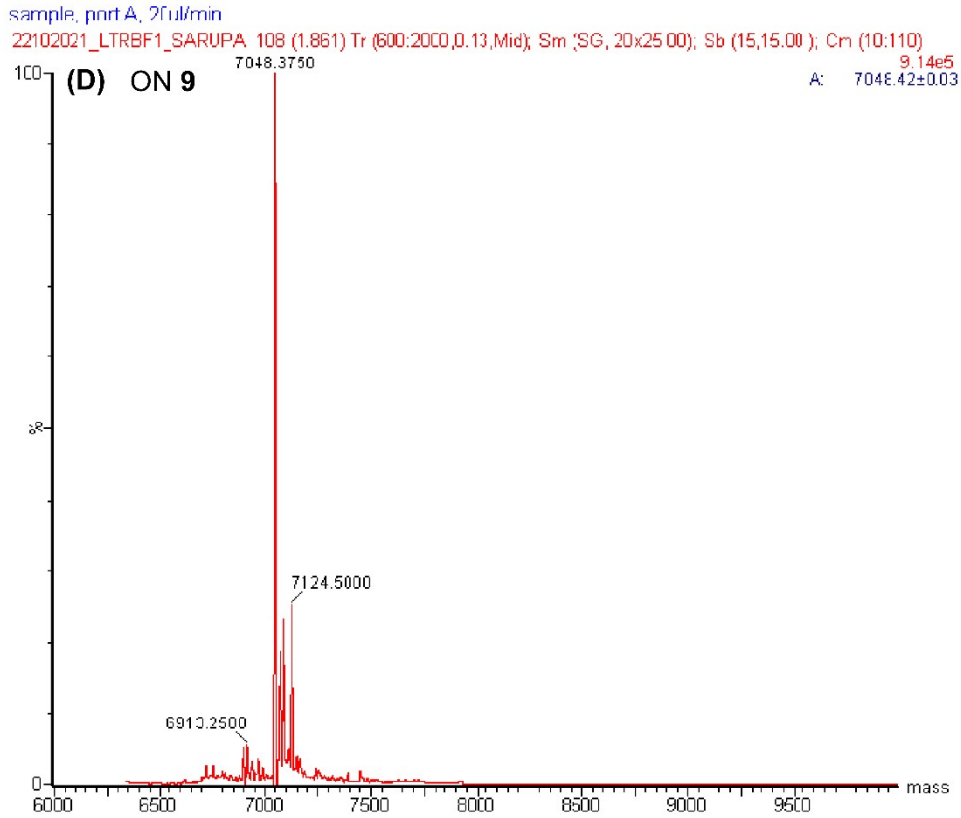
sample, port A, 20ul/min
22102021_LTRBF1_SARUPA 108 (1.861) Tr (600:2000,0.13,Mid); Sm (SG, 20x25.00); Sb (15,15.00); Cm (10:110)
(D) ON 9
9.14e5
A: 7048.42±0.03
7048.3750
7124.5000
6910.2500
mass

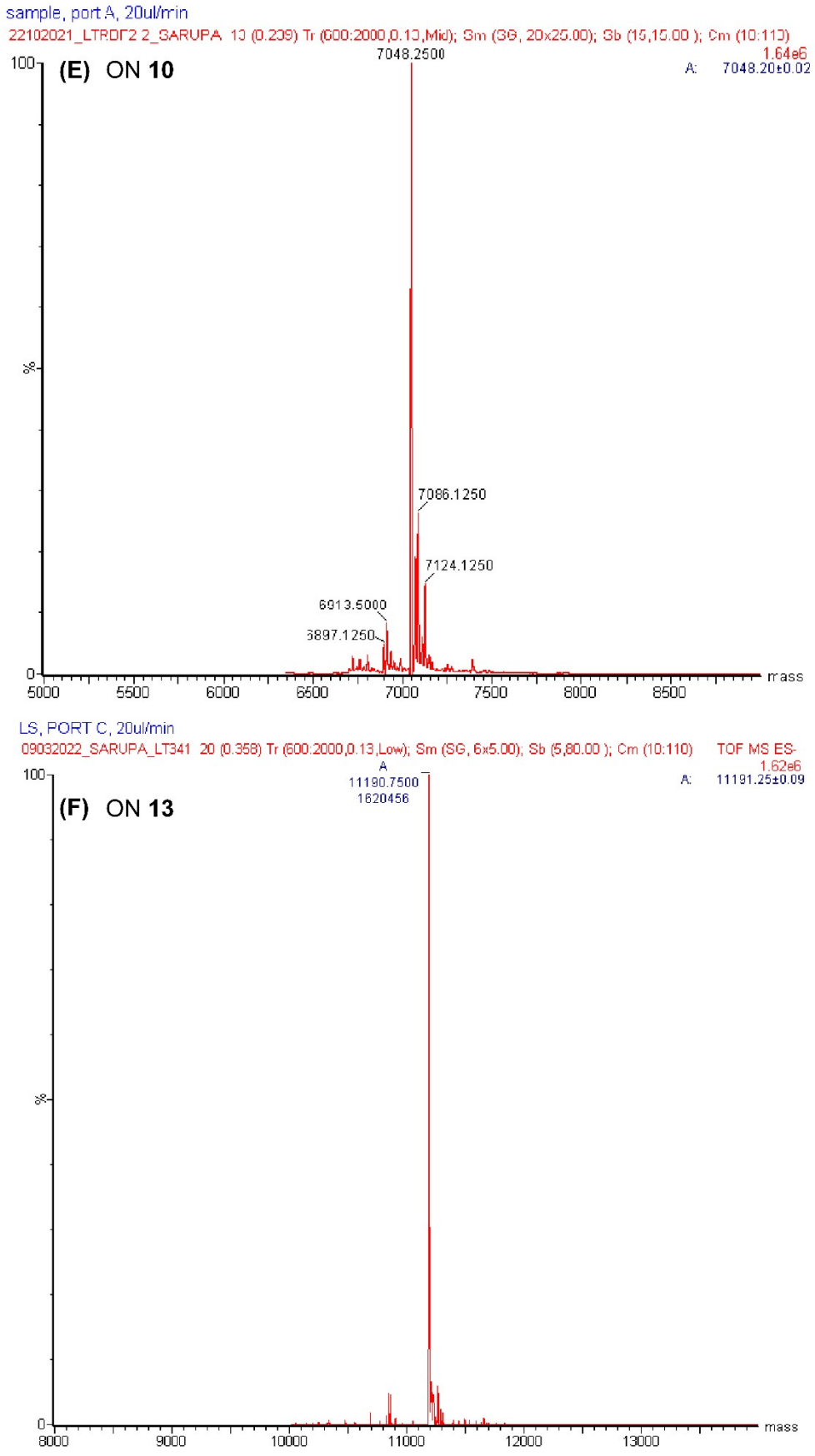
sample, port A, 20ul/min
22102021_LTRDF2 2_SARUPA 10 (0.239) Tr (600:2000,0.10,Mid); Sm (SG, 20x25.00); Sb (15,15.00); Cm (10:110)
1.64e6
A: 7048.20±0.02
(E) ON 10
7048.2500
7086.1250
7124.1250
6913.5000
3897.1250
100
%
0
5000
5500
6000
6500
7000
7500
8000
8500
mass
LS, PORT C, 20ul/min
09032022_SARUPA_LT341 20 (0.358) Tr (600:2000,0.13,Low); Sm (SG, 6x5.00); Sb (5,80.00); Cm (10:110)
TOF MS ES-
1.62e6
A: 11191.25±0.09
A
11190.7500
1620456
(F) ON 13
100
%
0
8000
9000
10000
11000
12000
13000
mass

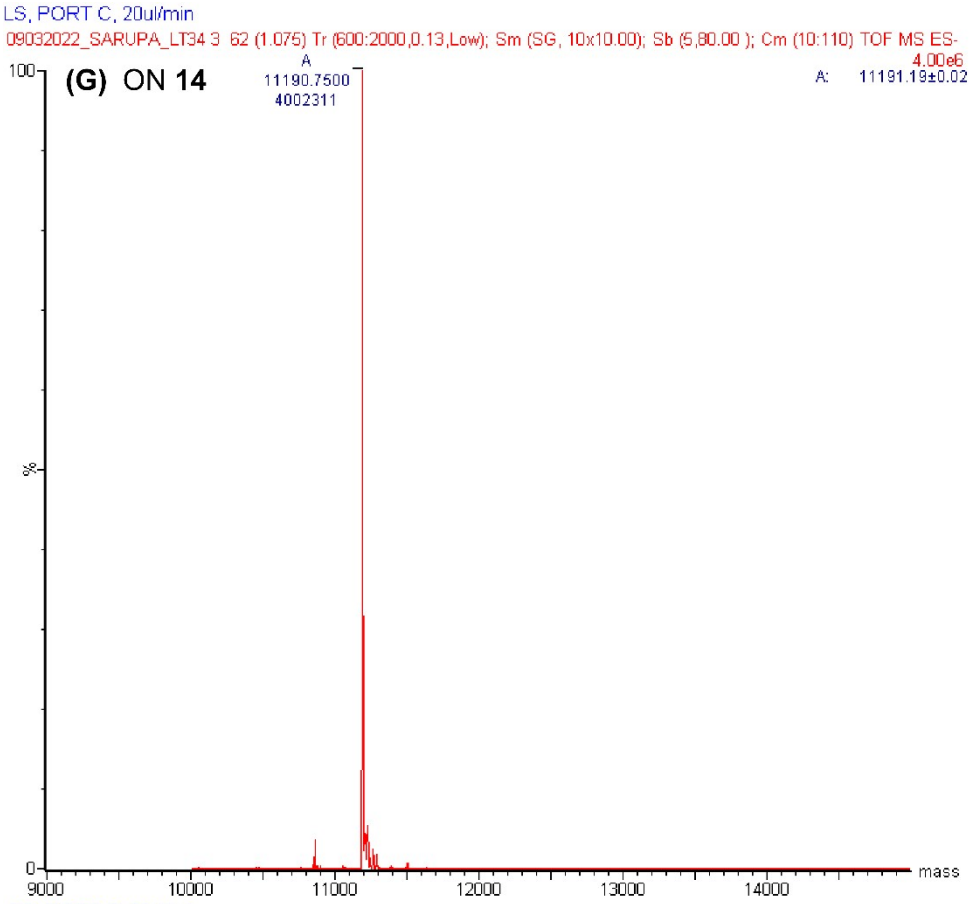
LS, PORT C, 20ul/min
09032022_SARUPA_LT34 3 62 (1.075) Tr (600:2000,0.13,Low); Sm (SG, 10x10.00); Sb (5,80.00); Cm (10:110) TOF MS ES-
4.00e6
(G) ON 14
A
11190.7500
4002311
A: 11191.19±0.02
100
%
0
9000
10000
11000
12000
13000
14000
mass

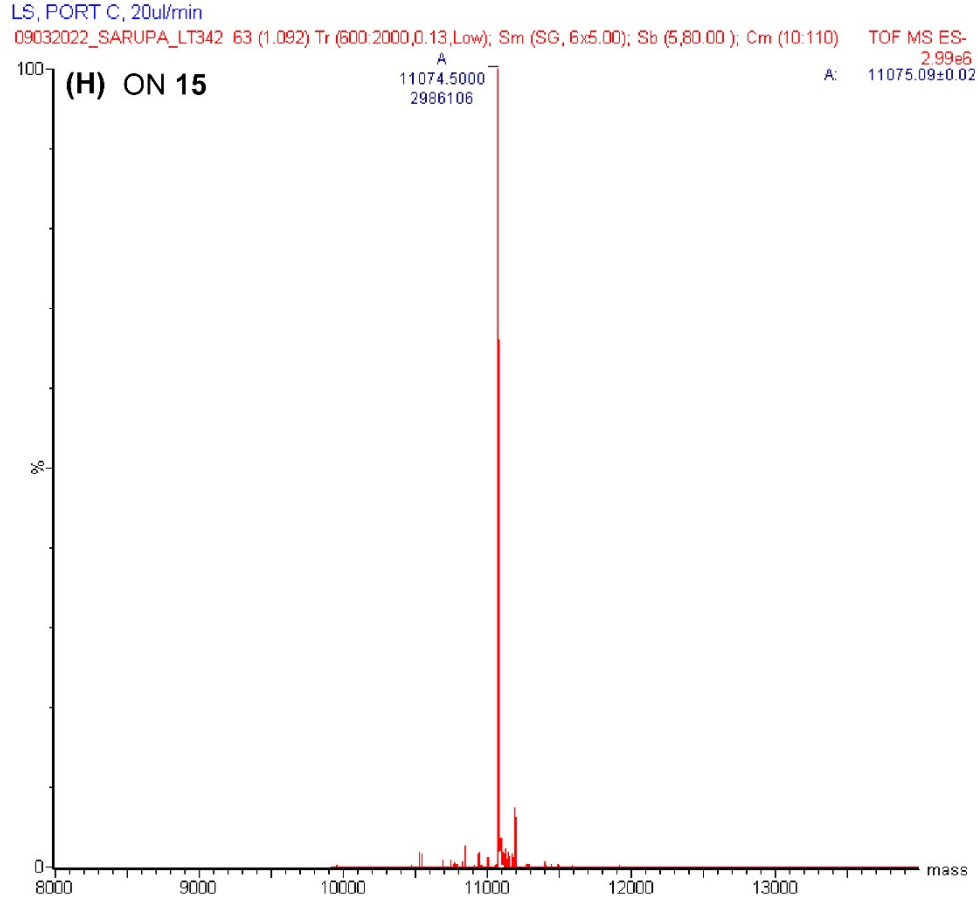
LS, PORT C, 20ul/min
09032022_SARUPA_LT342 63 (1.092) Tr (600:2000,0.13,Low); Sm (SG, 6x5.00); Sb (5,80.00); Cm (10:110)
TOF MS ES-
2.99e6
(H) ON 15
A
11074.5000
2986106
A: 11075.09±0.02
100
%
0
8000
9000
10000
11000
12000
13000
mass

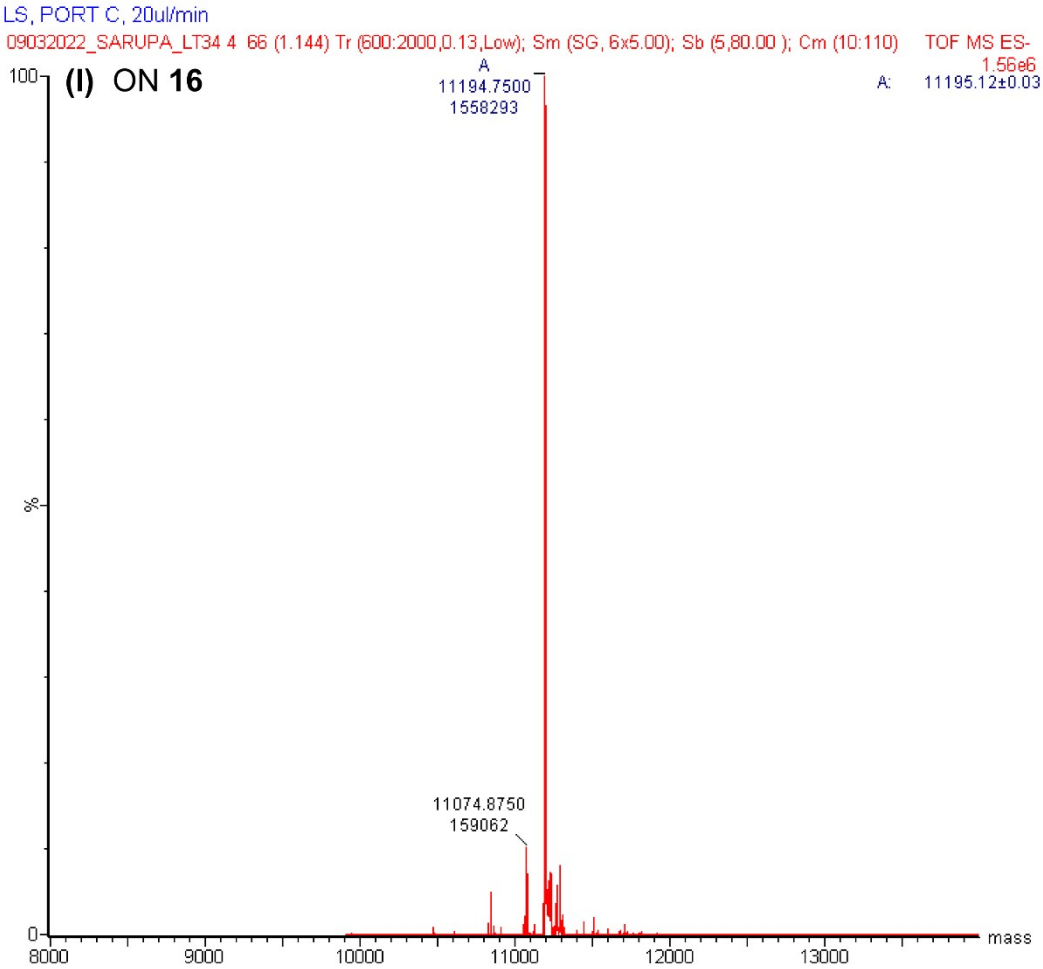

Fig. S2 ESI-MS of purified LTR ONs containing FBFdU and or FdU. See Table S1 for details.

Table S1. ε_{260} and mass data of modified LTR ONs

ON sequence	ε_{260} [M^{-1} cm^{-1}][a]	calculated (g/mol)	found (g/mol)
4	258418	8972.76	8972.75
5	268710	8968.79	8968.25
6	266087	8852.68	8852.75
9	212810	7048.58	7048.37
10	212810	7048.58	7048.25
13	342910	11191.23	11190.75
14	342910	11191.23	11190.75
15	348117	11075.11	11074.50
16	341896	11195.19	11194.75

[a]Molar absorption coefficient (ε) of modified ONs was determined by using OligoAnalyzer 3.1. The molar absorptivity of modified nucleosides FBFdU (ε_{260}= 10310 M^{-1} cm^{-1}) and FdU (ε_{260}= 7687 M^{-1} cm^{-1}) was used in place of dT.

5. Circular dichroism (CD) analysis: ONs **3**–**6**, **8**–**10** and **12**–**16** were annealed in 20 mM potassium phosphate buffer (pH 7) containing 70 mM KCl at 95 °C for 5 min and slowly cooled to RT. CD spectra were recorded from 320–200 nm at 25 °C using 1 nm bandwidth and sample volume of 200 µL using a quartz cuvette (Sterna Scientific, path length 2 mm) on a Jasco J-815 CD spectrometer. Each spectrum was recorded in duplicate with averaging three accumulations at scanning speed of 100 nm/min and baseline corrected for buffer contribution. Each spectrum was smoothened using the software provided by the manufacturer present in the system.

CD analysis in intraoocyte (IO) buffer: Control ON **12** (5 µM) and modified ON **16** (5 µM) were annealed in intraoocyte (IO) buffer (25 mM HEPES (pH 7.5), 10.5 mM NaCl, 110 mM KCl, 130 nM $CaCl_2$, 1 mM $MgCl_2$, 0.1 mM EDTA) at 95 °C for 5 minutes and allowed to cool at RT. CD spectra were recorded as mentioned above.

6. Thermal melting analysis: ONs **3**–**6**, **8**–**10** and **12**–**16** were annealed in 20 mM potassium phosphate buffer (pH 7) containing 70 mM KCl as mentioned above. The spectra were recorded in Cary 300 Bio UV–Vis spectrophotometer for ONs **3**–**6** and ONs **12**–**16**. Cary 3500 multicell UV-Vis spectrophotometer was used for recording the spectra for ONs **8**–**10** with a temperature interval of 1 °C. Absorbance was recorded at 295 nm with a data interval of 1 °C for ONs **3**–**6**, ONs **12**–**16** and 0.5 °C for ONs **8**–**10**.

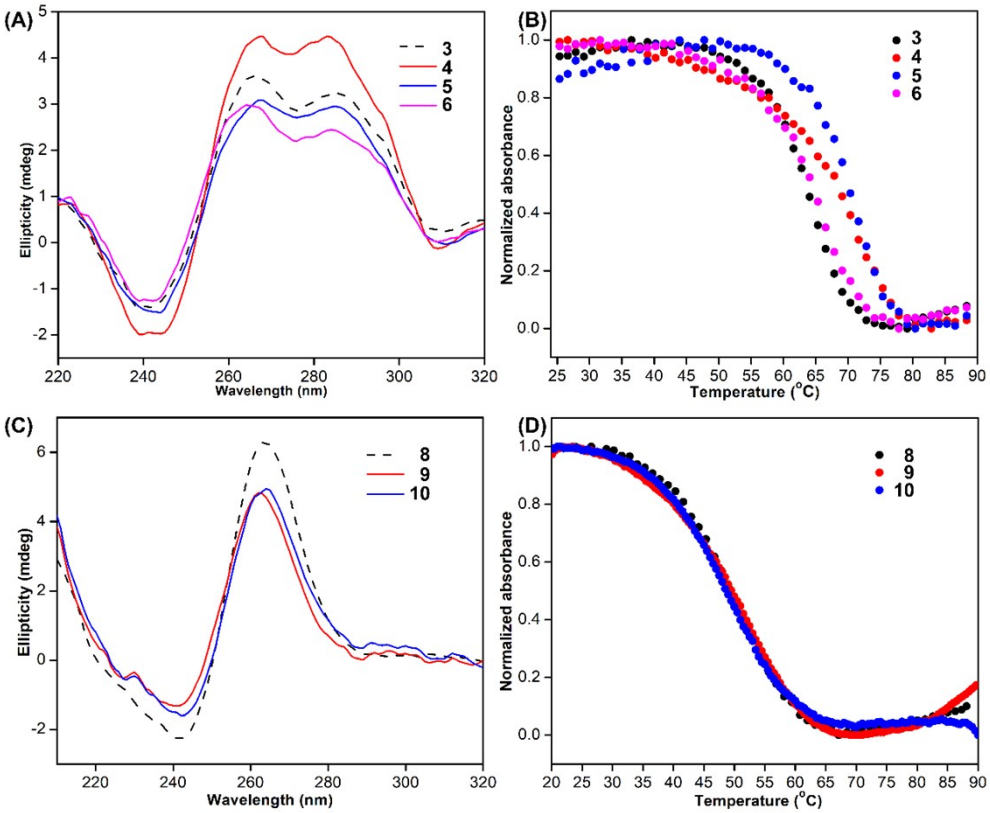

Fig. S3 (**A**) CD spectra of control LTR-III ON **3** (5 µM), modified LTR-III ONs **4**–**6** (5 µM). (**B**) UV-thermal melting profiles for the same at 295 nm (2 µM). (**C**) CD spectra of control LTR-IV ON **8** (8 µM), modified LTR-IV ONs **9** and **10** (8 µM). (**D**) UV-thermal melting profiles for the same at 295 nm (5 µM). See Table S2 for T_m values.

Table S2. T_m values of modified and control unmodified ONs.[a]

	LTR-III ONs	T_m (°C)	LTR-IV ONs	T_m (°C)	LTR-III + IV ONs	T_m (°C)
control unmodified ONs	**3**	65.0 ± 0.7	**8**	51.6 ± 0.3	**12**	55.6 ± 0.2
modified ONs	**4**	69.4 ± 1.6	**9**	52.2 ± 0.7	**13**	60.6 ± 0.3
	5	69.0 ± 1.7	**10**	51.6 ± 1.2	**14**	55.6 ± 0.4
	6	64.8 ± 0.7			**15**	56.5 ± 0.3
					16	55.2 ± 0.4

[a] Standard deviation reported from triplicate measurements.

7. Steady-state fluorescence of modified LTR ONs: LTR GQ structures of ONs **4** (0.5 μM), **9** (1 μM) and **10** (1 μM) were formed by heating the samples at 95 °C for 5 min in 20 mM potassium phosphate buffer (pH 7) containing 70 mM KCl. The corresponding duplexes **4•7**, **9•11** and **10•11** were prepared by heating a 1:1.1 mixture of LTR ONs **4**, **9** and **10** with complementary ONs **7** and **11** at 95 °C for 5 min in the same ionic conditions as mentioned above. All the samples were cooled slowly to RT. Experiments were done in triplicate in a micro-fluorescence cuvette (Hellma, path length 1.0 cm) on a Fluoromax-4 spectrofluorometer (Horiba Scientific) at 25 °C.

8. NMR of LTR ONs: LTR GQ structures of ONs **3**–**6** (45 μM), **8** (75 μM), **9** (10 μM or 75 μM), **10** (75 μM), **13**–**16** (45 μM) were formed by heating the samples at 95 °C for 5 min in 20 mM potassium phosphate buffer (pH 7) containing 70 mM KCl in 20% D_2O. The corresponding duplexes **4•7** and **9•11** were prepared by heating a 1:1.1 mixture of LTR ONs **4** and **9** with complementary ONs **7** and **11** respectively at 95 °C for 5 min in the same ionic conditions as mentioned above. ^{19}F and ^{1}H NMR spectra were acquired at a frequency of 564.9 MHz and 600 MHz, respectively, on a Bruker AVANCE III HD ASCEND 600 MHz spectrometer equipped with CryoProbe (CP2.1 QCl 600S3 H/F-C/N-D-05 Z XT). All ^{19}F NMR spectrum were calibrated relative to an external standard, trifluorotoluene (TFT = −63.72 ppm). Spectral parameters for ^{19}F NMR: excitation pulse: 12 μs; spectral width: 90.32 ppm; transmitter frequency offset: -145 ppm; acquisition time: 0.33 s; relaxation delay: 1.0 s; number of scans: 5000–6000. Using these parameters, spectra were obtained in 2–2.5 h. Each spectrum was processed with an exponential window function using lb = 20 Hz. ^{1}H NMR spectra were obtained with water suppression using excitation sculpting with gradients. Number of scans was 1200.

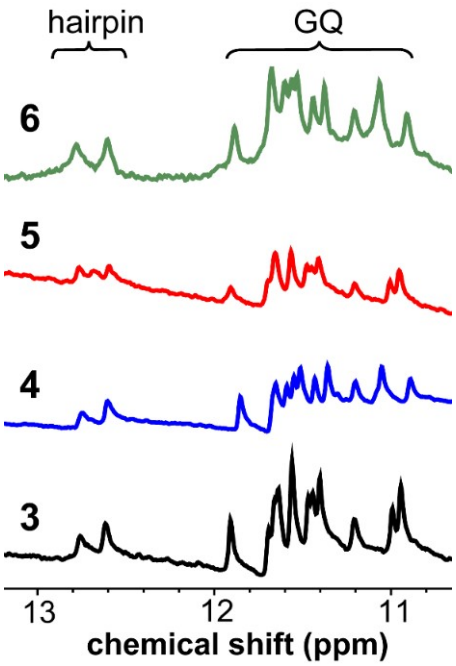

Fig. S4 Partial ^{1}H NMR spectra (45 µM) of control ON **3** and modified ONs **4**–**6**. For details see Section 8.

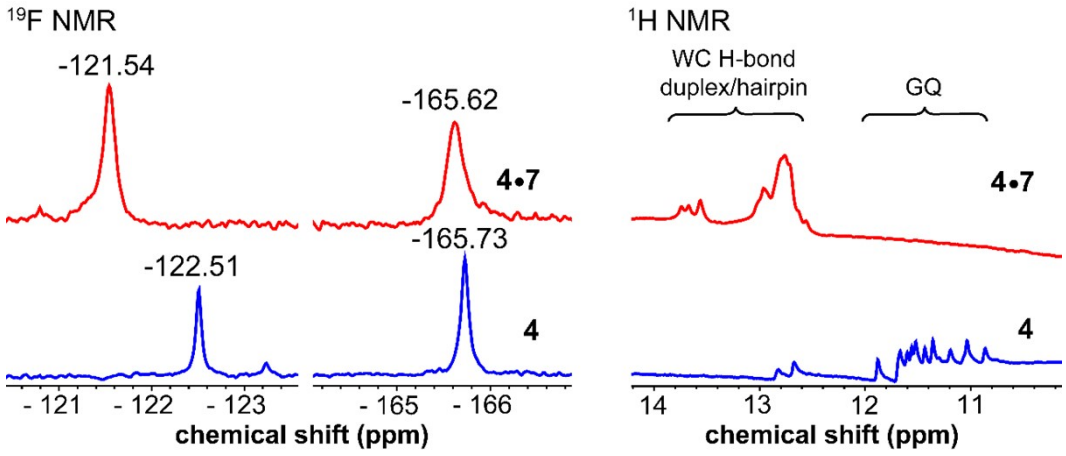

Fig. S5 ^{19}F and ^{1}H NMR spectra (45 µM) of ON **4** and its duplex **4•7**. For details see Section 8.

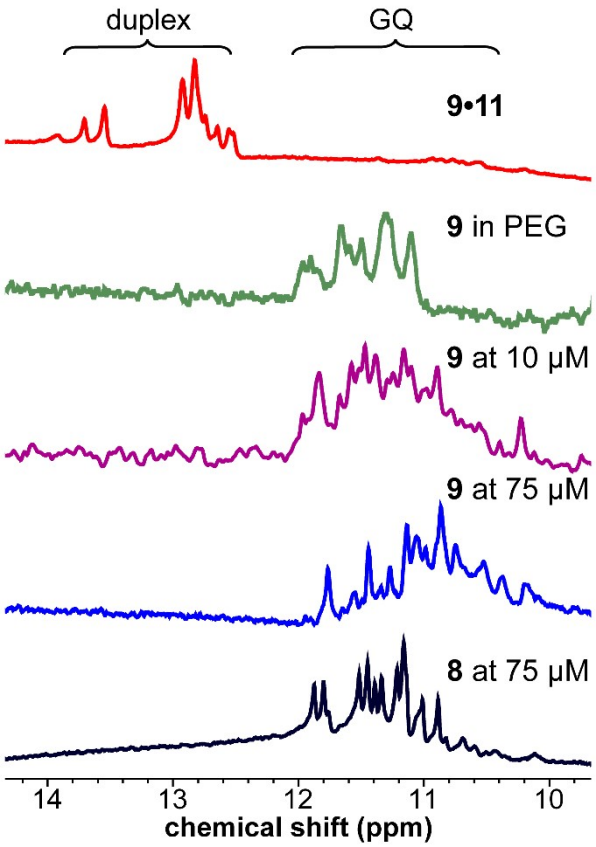

Fig. S6 Partial ^{1}H NMR spectra of control ON **8** (75 µM) and FBFdU-modified ON **9** under different conditions. For details see Section 8.

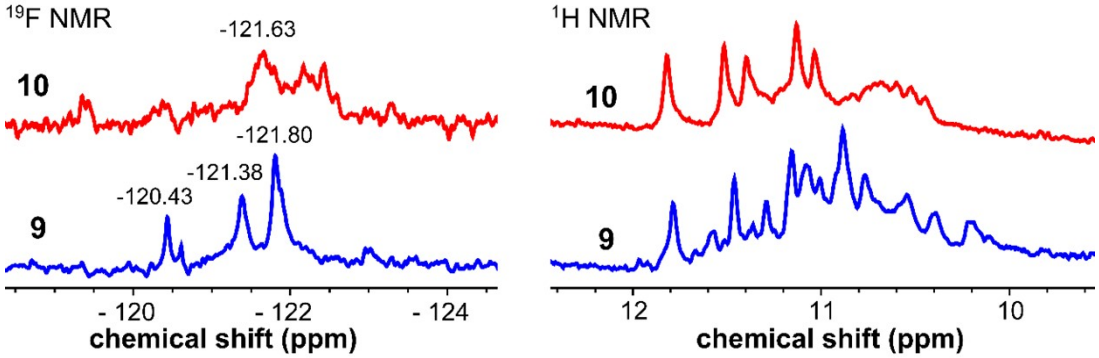

Fig. S7 ^{19}F and ^{1}H NMR spectra of ONs **9** and **10.** For details see Section 8.

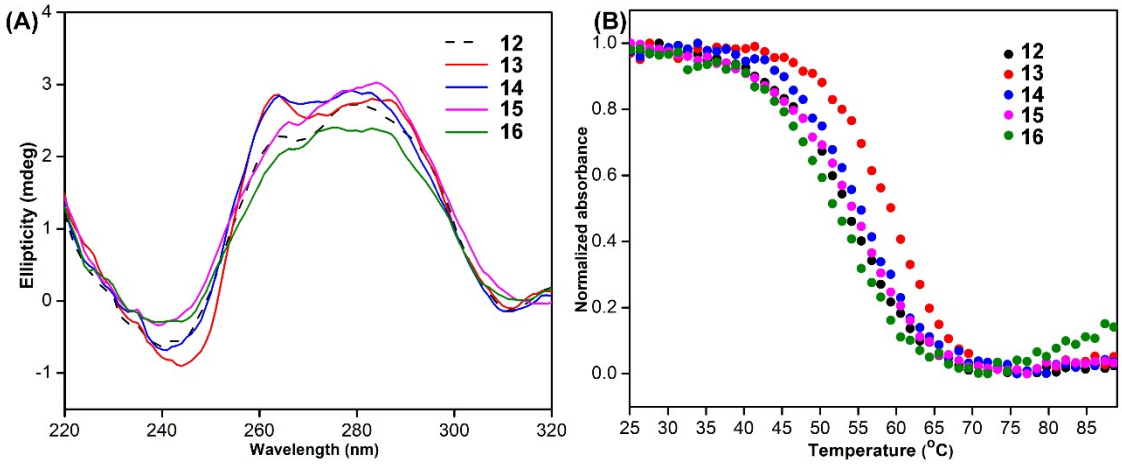

Fig. S8 (**A**) CD spectra of control LTR-(III+IV) ON **12** (5 µM), modified LTR-(III+IV) ONs **13**–**16** (5 µM). (**B**) UV-thermal melting profiles for the same at 295 nm (2 µM). See Section 5 and 6 for experimental details

9. Preparation of ON 16 for ^{19}F NMR analysis in intraoocyte buffer, lysate and egg extract.

An adult female *Xenopus laevis* was anesthetized and its oocytes were surgically removed following the protocol approved by the Institutional Animal Ethics Committee (IAEC), Indian Institute of Science Education and Research (IISER) Bhopal. All experiments that employed *Xenopus laevis* oocytes were performed in accordance with a protocol approved by the Institutional Animal Ethics Committee (IAEC) (proposal application number 2023-IISERB-01-IEAC), IISER Bhopal following the guidelines prescribed by the Committee for the Purpose of Control and Supervision of Experiments on Animals (CPCSEA), Government of India.

In IO buffer: ^{1}H NMR and ^{19}F NMR spectra of ON **16** (100 µM) annealed in IO buffer containing 20% D_2O were recorded at a frequency of 564.9 MHz and 600 MHz (25 °C), respectively. Spectral parameters are the same as mentioned in Section 8. ^{19}F NMR (number of scans = 6000) and ^{1}H NMR (number of scans = 1500). ^{19}F NMR spectra were processed with an exponential window function using lb = 20 Hz.

In egg lysate: Near 280 healthy *Xenopus laevis* oocytes (stage V/VI) were selected and kept in an ice-cold petri-dish containing 15 mL of Ori-Ca^{2+} buffer (5 mM HEPES (pH 7.5), 110 mM NaCl, 5 mM KCl, 2 mM $CaCl_2$, and 1 mM $MgCl_2$) for 15 min. Oocytes were washed with ice-cold Ori-Ca^{2+} buffer (15 mL). The buffer was removed and oocytes were resuspended in IO buffer (15 mL, 15 min). This step was repeated two more times. Oocytes were transferred to a centrifuge tube and allowed to settle down. The excess buffer was removed carefully without disturbing the settled oocytes. Oocytes were again washed with 200 µL of IO buffer containing 20% D_2O (repeated two times). Eggs were finally resuspended in 200 µL of IO buffer containing 20% D_2O and mechanically crushed. The suspension was centrifuged at 20000g (at 4 °C) for 10 min. The interphase layer was transferred to another centrifuge tube and heat denatured at 95 °C for 10 min. The sample was centrifuged at 20000g (4 °C, 10 min) and the clear lysate (300 µL) was transferred to another centrifuge tube and stored at 4 °C. ON **16** (1 mM, 30 µL) annealed in IO buffer containing 20% D_2O was added to the clear lysate (270 µL) and mixed well. The final sample volume was 300 µL containing 100 µM of the ON. The sample was incubated for 30 min at 4 °C

and then brought to 25 °C before recording the NMR using following parameters. ^{19}F NMR (number of scans = 6000) and ^{1}H NMR (number of scans = 1500) spectra were acquired at a frequency of 564.9 MHz and 600 MHz (25 °C), respectively. Spectral parameters are the same as mentioned in Section 8. ^{19}F NMR spectra were processed with an exponential window function using lb = 20 Hz. After the analysis, the sample was stored at -20 °C and analyzed by RP-HPLC to study the integrity of the ON in cell lysate during the NMR acquisition time. Sample was filtered using a centrifuge spin filter. The centrifuge tube was washed with 50 µL of water. The combined solution was analyzed by RP-HPLC and the fraction corresponding to ON **16** was further analyzed by ESI-MS (Figure S11 and S12).

In egg extract: 850–900 healthy oocytes were transferred into a petri-dish containing cold Ori-Ca^{2+} buffer (15 mL) and kept for 15–20 min. The eggs were then shifted to another petri-dish containing ice-cold IO buffer and incubated for 15 min. The oocytes were washed with ice-cold IO buffer (2 x 15 mL) and transferred to a centrifuge tube. Buffer above the oocytes was removed carefully after they settled down. Oocytes were washed with IO buffer (400 µL) containing 20% D_2O (repeated two times). After the centrifugation of the oocytes at 400g for 1 min at 4 °C, the supernatant buffer was removed carefully. The oocytes were again supplemented with intraoocyte buffer (100 µL) containing 20% D_2O and centrifuged at 12000g for 5 min at 4 °C. The eggs were crushed mechanically and the suspension was centrifuged at 12000g for 30 min at 4 °C to obtain the interphase layer. This crude interphase layer was directly used for the NMR analysis. 2 mM of the preannealed ON **16** (15 µL) in IO buffer containing 20% D_2O was added to the above crude egg extract (285 µL) and incubated for 30 min at 4 °C. The final sample volume was 300 µL containing 100 µM of the ON. The ^{19}F (number of scans = 6000) and ^{1}H NMR (number of scans = 4000) spectra were recorded at a frequency of 564.9 MHz and 600 MHz at 25 °C, respectively. Spectral parameters are the same as mentioned above. The ^{19}F NMR spectrum was processed with an exponential window function using lb = 20 Hz.

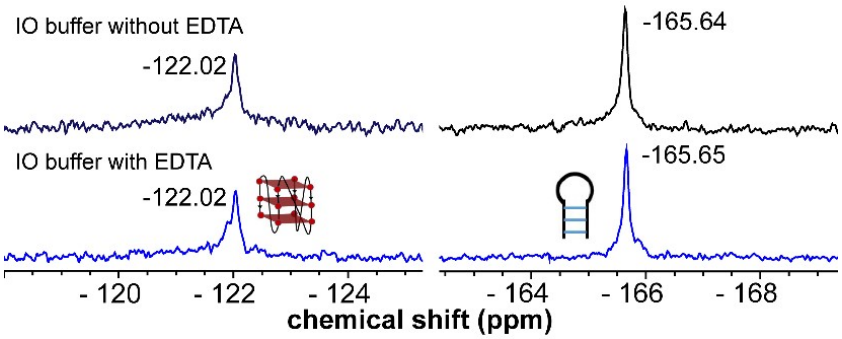

Fig. S9 ^{19}F NMR of ON **16** (100 µM) in IO buffer without EDTA (black line) and IO buffer with EDTA (blue line). We obtained peaks with almost the same chemical shifts in the absence and presence of EDTA. In NMR experiments with frog egg lysate and extract we used a small amount of EDTA as it is usually used in intracellular and lysis buffers to reduce the degradation of DNA from nucleases.[S4,S5] It is to be noted that the presence or absence of EDTA did not affect the NMR analysis.

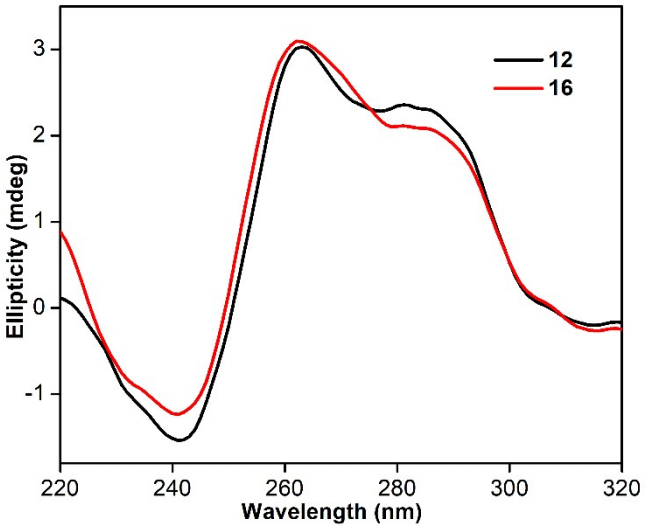

Fig. S10 CD spectra of ONs **12** and **16** each at 5 µM in intraoocyte (IO) buffer. See Section 5 for details.

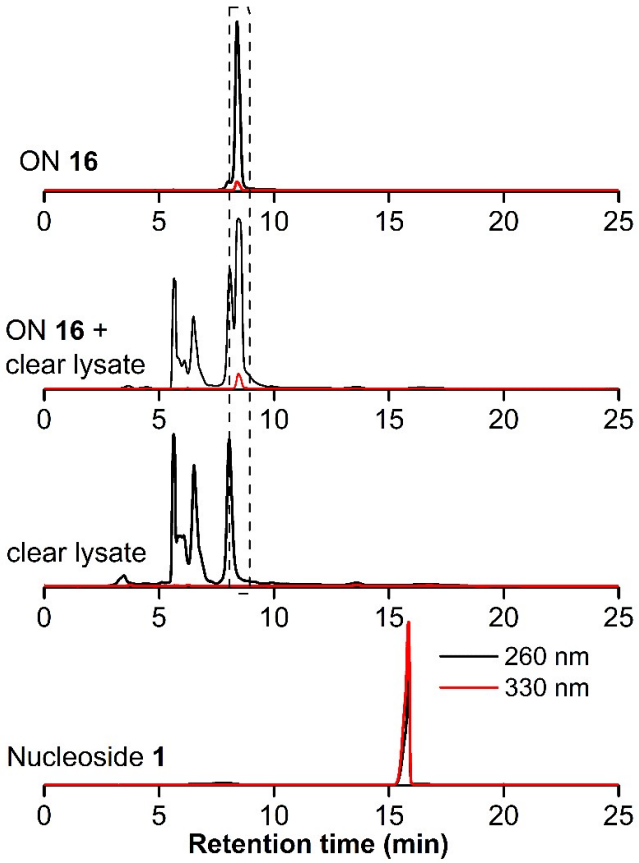

Fig. S11 Comparison of RP-HPLC chromatogram of ON **16**, **16** in lysate after the NMR experiments, lysate (control) and nucleoside FBFdU **1** at 260 nm and 330 nm. ON **16** is stable in the lysate and no detectable degradation of ON **16** was observed (see the peak within the dashed line). Peaks between 5–8 min are from metabolites of the clear lysate.

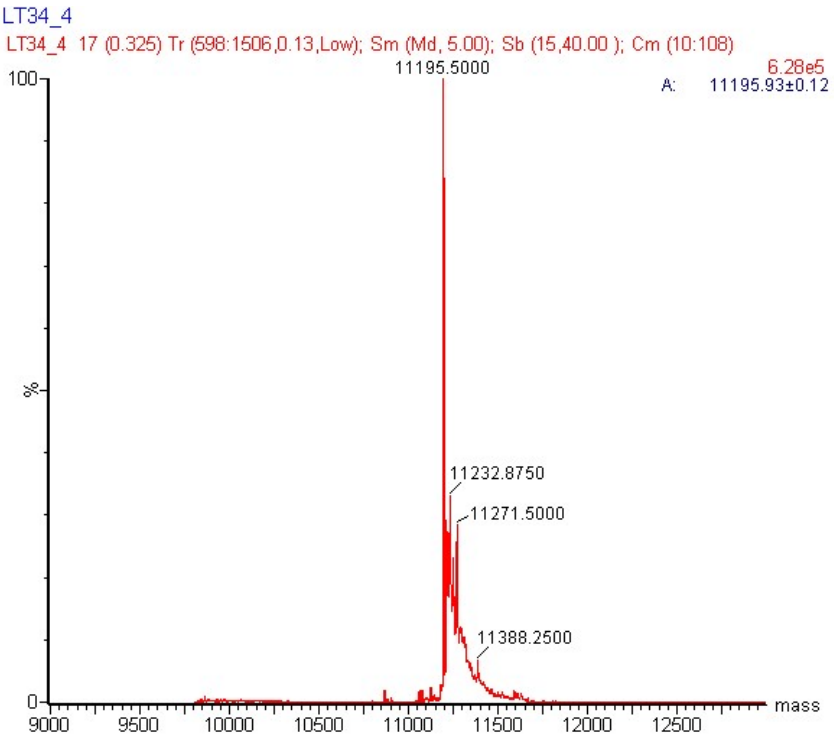

Fig. S12 ESI-MS spectra of modified ON **16** extracted from lysate sample after NMR analysis (calculated mass = 11194.75, observed mass =11195.50).

Table S3. Absorbance and emission wavelengths of nucleoside FBFdU (**1**) in different solvents. Data reported from J. Am. Chem. Soc. 2018, 140, 12622–12633.[S1]

solvent	λ_{max} (nm)	λ_{em} (nm)	Φ
water	322	437	0.11
methanol	322	418	0.04
dioxane	324	400	0.03
ethylene glycol	325	420	0.20
glycerol	326	424	0.52

Table S4. ^{19}F NMR chemical shift (ppm) of FBFdU (**1**) and FdU (**2**) in different solvents.[S1, S2]
Although ^{19}F label exhibits distinct chemical shifts in different solvents, the trend based on polarity and viscosity order is complex.

solvent	FBFdU	FdU
water	-121.78	-166.49
methanol	-123.70	-169.39
dioxane	-123.01	-169.06
ethylene glycol	-122.35	-168.05

10. Computational analysis: Molecular dynamics (MD) simulations were carried out using the templates HIV LTR-III (PDB ID: 6H1K)[S6] LTR-IV (PDB ID:2N4Y)[S7]. Force field parameters were generated for FdU and FBFdU to prepare the ON structures with the probes. Both structures were prepared using GaussView 6.0 with phosphate capping at both 3' and 5' ends. FBFdU has a rotatable bond between the fluorophore and the base. A dihedral scan was performed for FBFdU with 36 rotations of 10 degrees each in Gaussian 16 version B.01[S8] at theory

level HF/6-31G* to find the most stable conformer. The stable conformer showing the lowest potential energy was then optimized in Gaussian 16 at the same theory level. FdU was also optimized using a similar strategy. ESP charges were calculated using Gaussian 16, and RESP fitting was done in the antechamber[S9] module of AmberTools 19. The parmchk2 program generated an initial set of force field parameters. However, some were missing parameters, and others had high penalty scores. The capping was then removed, and after fixing the overall charges, the GAFF[S10] library was used to fill in the missing parameters. Finally, prepin files were generated for complex preparation.

These modifications were incorporated into their respective templates in tleap. Central K^+ of the GQ core was also added using manual coordinate calculations. The complex was solvated with a rectangular water box using TIP3PBOX force field having an edge length of 10 Å. ~27 K^+ were added to neutralize the system. OL15[S11] was used to define the DNA. MD simulations were carried out using our previously reported protocol.[S10] Briefly, all the complexes were subjected to 10,000 steps of restrained minimization by the steepest descent method with a restraint of 2.0 kcal/mol. $Å^2$ followed by 100 ps of heating and 100 ps of density equilibration. Further, 800 ps of NPT equilibration and 500 ns of production run were carried out in GPU accelerated version of PMEMD[S13-S15] in AMBER 18.[S16] A total of ~2.5 µs (5*500 ns) simulations were carried out. The SHAKE algorithm was applied to subject the hydrogens to bond length constraints. All the MD analyses were carried out using the CPPTRAJ[S17] module of AmberTools 19. The hierarchical agglomerative algorithm was used for clustering the trajectories. The cut-offs for stacking were a COM distance of 5 Å and a vector angle of 45 degrees. The trajectories were visualized using VMD,[S16] and images were rendered using PyMOL(Schrodinger LLC.)

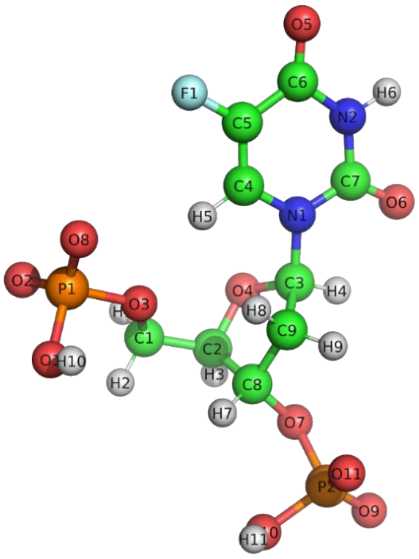


```
     0    0              2
   This is a remark line
molecule.res
   FDU             INT         0
   CORRECT         OMIT        DU       BEG
        0.0000
        1   DUMM    DU    M    0    -1    -2     0       0       0       0
        2   DUMM    DU    M    1    0     -1     1.449   0       0       0
        3   DUMM    DU    M    2    1     0      1.523   111.21  0       0
```

4	P1	P	M	3	2	1	1.54	111.208	-180	1.294462
5	O2	O2	E	4	3	2	1.469	81.307	-120.503	-0.909793
6	O8	O2	E	4	3	2	1.472	46.311	76.917	-0.909793
7	O3	OS	M	4	3	2	1.646	110.787	-13.801	-0.640503
8	C1	CT	M	7	4	3	1.398	120.517	-120.842	0.144315
9	H1	H1	E	8	7	4	1.083	110.027	63.971	0.038448
10	H2	H1	E	8	7	4	1.086	110.759	-55.331	0.038448
11	C2	CT	M	8	7	4	1.516	109.506	-175.355	0.10031
12	H3	H1	E	11	8	7	1.083	108.884	179.331	0.068969
13	O4	OS	S	11	8	7	1.426	109.53	-62.744	-0.471067
14	C3	CT	3	13	11	8	1.392	111.377	121.413	0.280157
15	H4	H2	E	14	13	11	1.075	110.454	103.214	0.089924
16	N1	N*	S	14	13	11	1.474	108.136	-141.827	-0.385478
17	C4	CM	B	16	14	13	1.383	119.469	52.773	0.047923
18	H5	H4	E	17	16	14	1.075	116.654	3.002	0.233236
19	C5	CM	B	17	16	14	1.328	121.991	-176.865	-0.094409
20	C6	C	B	19	17	16	1.45	121.491	0.422	0.642038
21	O5	O	E	20	19	17	1.2	127.066	179.948	-0.707254
22	N2	NA	B	20	19	17	1.38	111.743	0.057	-0.646274
23	H6	H	E	22	20	19	0.997	116.47	179.661	0.304756
24	C7	C	S	22	20	19	1.379	128.863	0.555	0.73023
25	O6	O	E	24	22	20	1.2	119.961	178.871	-0.727943
26	F1	F	E	19	17	16	1.327	122.327	179.93	-0.148638
27	C9	CT	B	14	13	11	1.524	106.529	-18.129	-0.132195
28	H8	HC	E	27	14	13	1.082	110.583	-84.598	0.063958
29	H9	HC	E	27	14	13	1.08	113.265	151.624	0.063958
30	C8	CT	M	11	8	7	1.537	115.49	56.62	0.179574
31	H7	H1	E	30	11	8	1.081	111.369	22.658	0.078991
32	O7	OS	M	30	11	8	1.402	107.933	144.829	-0.626347
LOOP										
C7	N1									
C8	C9									
IMPROPER										
C7	C4	N1	C3							
C5	H5	C4	N1							
C6	C4	C5	F1							
C5	N2	C6	O5							
C6	C7	N2	H6							
N1	N2	C7	O6							
DONE										
STOP										

Fig. S13 Cartesian coordinates and RESP charges calculated for the FdU adduct generated using Gaussian 16. Carbons atoms are represented by green, nitrogen atoms by blue, oxygen atoms by red, fluorine by cyan and hydrogen atoms by white respectively.

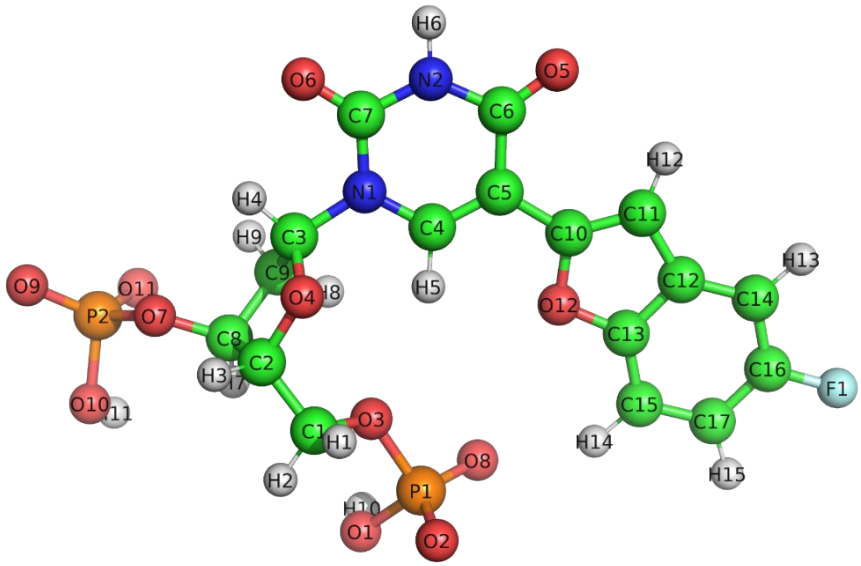

0	0	2								
This is a remark line										
molecule.res										
FBFDU	INT	0								
CORRECT	OMIT	DU	BEG							
0.0000										
1	DUMM	DU	M	0	-1	-2	0	0	0	0
2	DUMM	DU	M	1	0	-1	1.449	0	0	0
3	DUMM	DU	M	2	1	0	1.523	111.21	0	0
4	P1	P	M	3	2	1	1.54	111.208	-180	1.329951
5	O2	O2	E	4	3	2	1.469	102.542	-69.037	-0.907294
6	O8	O2	E	4	3	2	1.477	133.025	105.246	-0.907294
7	O3	OS	M	4	3	2	1.644	57.297	-173.44	-0.629415
8	C1	CT	M	7	4	3	1.402	118.04	54.604	0.143944
9	H1	H1	E	8	7	4	1.084	109.87	71.765	0.042331
10	H2	H1	E	8	7	4	1.086	110.559	-47.174	0.042331
11	C2	CT	M	8	7	4	1.514	110.845	-167.033	0.101983
12	H3	H1	E	11	8	7	1.083	108.375	176.116	0.071046
13	O4	OS	S	11	8	7	1.429	109.832	-66.203	-0.463418
14	C3	CT	3	13	11	8	1.391	110.667	128.117	0.279273
15	H4	H2	E	14	13	11	1.077	111.028	96.849	0.094203
16	N1	N*	S	14	13	11	1.475	107.506	-147.989	-0.379024
17	C4	CM	B	16	14	13	1.364	119.403	52.105	0.123751
18	H5	H4	E	17	16	14	1.075	114.89	2.014	0.233422
19	C5	CM	B	17	16	14	1.35	123.996	-177.596	-0.298709
20	C6	C	B	19	17	16	1.455	118.481	1.281	0.680537
21	O5	O	E	20	19	17	1.202	127.194	179.279	-0.708119
22	N2	NA	B	20	19	17	1.381	113.242	-0.56	-0.638327
23	H6	H	E	22	20	19	0.997	116.23	179.821	0.311693
24	C7	C	S	22	20	19	1.373	128.831	0.532	0.743339
25	O6	O	E	24	22	20	1.197	120.755	179.188	-0.707045
26	C10	C*	S	19	17	16	1.461	121.17	-178.289	0.120509
27	C11	C*	B	26	19	17	1.347	133.367	-175.809	-0.216033
28	C12	CB	S	27	26	19	1.446	105.519	-179.349	-0.092125
29	C13	CB	B	28	27	26	1.389	105.35	0.092	0.052891
30	C15	CA	B	29	28	27	1.38	124.347	179.52	-0.068718
31	C17	CA	B	30	29	28	1.38	116.104	0.291	-0.19327
32	C16	CA	B	31	30	29	1.39	119.966	-0.033	0.074936
33	C14	CA	S	32	31	30	1.372	123.833	-0.186	-0.165353

34	H13	HA	E	33	32	31	1.075	120.429	-179.75	0.122269
35	F1	F	E	32	31	30	1.346	117.813	-179.963	-0.18672
36	H15	HA	E	31	30	29	1.074	121.136	179.921	0.1269
37	H14	HA	E	30	29	28	1.078	119.977	-179.04	0.228791
38	O12	OS	E	29	28	27	1.35	109.737	-0.162	-0.17201
39	H12	HA	E	27	26	19	1.066	125.988	0.284	0.160246
40	C9	CT	B	14	13	11	1.522	105.968	-24.509	-0.132497
41	H8	HC	E	40	14	13	1.083	110.505	-79.957	0.065488
42	H9	HC	E	40	14	13	1.079	113.784	155.703	0.065488
43	C8	CT	M	11	8	7	1.538	115.921	53.869	0.183496
44	H7	H1	E	43	11	8	1.081	111.413	19.034	0.083087
45	O7	OS	M	43	11	8	1.401	107.861	141.357	-0.616531
LOOP										
C7	N1									
O12	C10									
C14	C12									
C8	C9									
IMPROPER										
C7	C4	N1	C3							
C5	H5	C4	N1							
C10	C6	C5	C4							
C5	N2	C6	O5							
C6	C7	N2	H6							
N1	N2	C7	O6							
C11	C5	C10	O12							
C10	C12	C11	H12							
C11	C14	C12	C13							
C15	C12	C13	O12							
C17	C13	C15	H14							
C15	C16	C17	H15							
C17	C14	C16	F1							
C16	C12	C14	H13							
DONE										
STOP										

Fig. S14 Cartesian coordinates and RESP charges calculated for the FBFdU adduct generated using Gaussian 16. Carbons atoms are represented by green, nitrogen atoms by blue, oxygen atoms by red, fluorine by cyan and hydrogen atoms by white respectively.

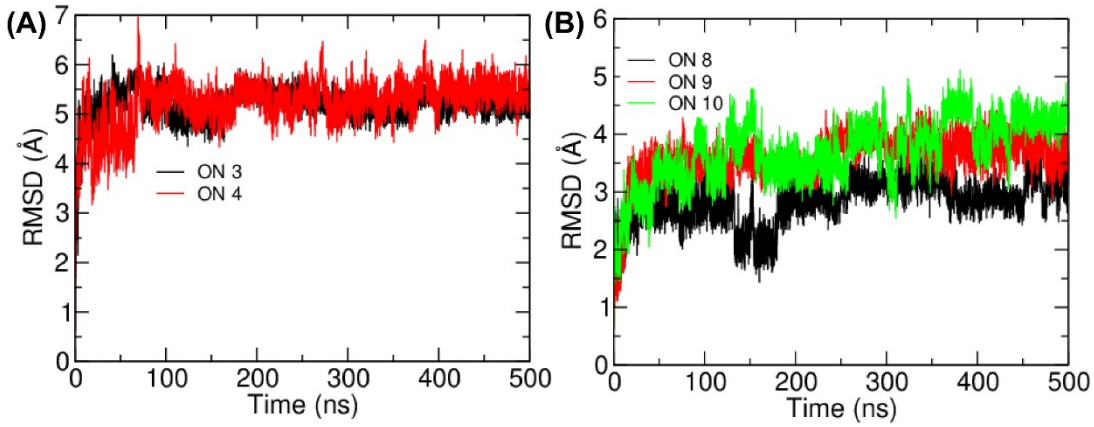

Fig. S15 RMSD plot of (**A**) LTR-III ON **3** and ON **4** (**B**) LTR-IV ON **8**, ON **9** and ON **10**. RMSD values were calculated from the 500 ns MD simulations.

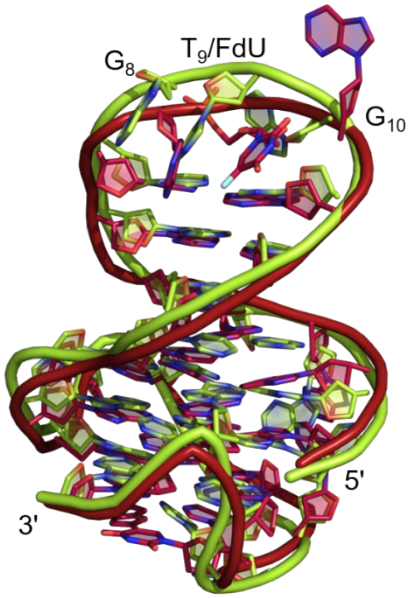

Fig. S16 Superimposed images of the major clusters of LTR-III native ON **3** and modified ON **4**. ON **3** and **4** are represented in green and maroon, respectively. The bases, which show maximum changes in the orientation are labeled in the Figure. The clusters have been obtained from the 500 ns MD simulation. The incorporation of FdU results in the partial stacking of FdU with G_8 and alters the orientation slightly from the native form while FBFdU remains the same. Model for ON **4** is available with the private link and access code (password): https://www.modelarchive.org/doi/10.5452/ma-okc7y
Code: QwwKvEyOwE

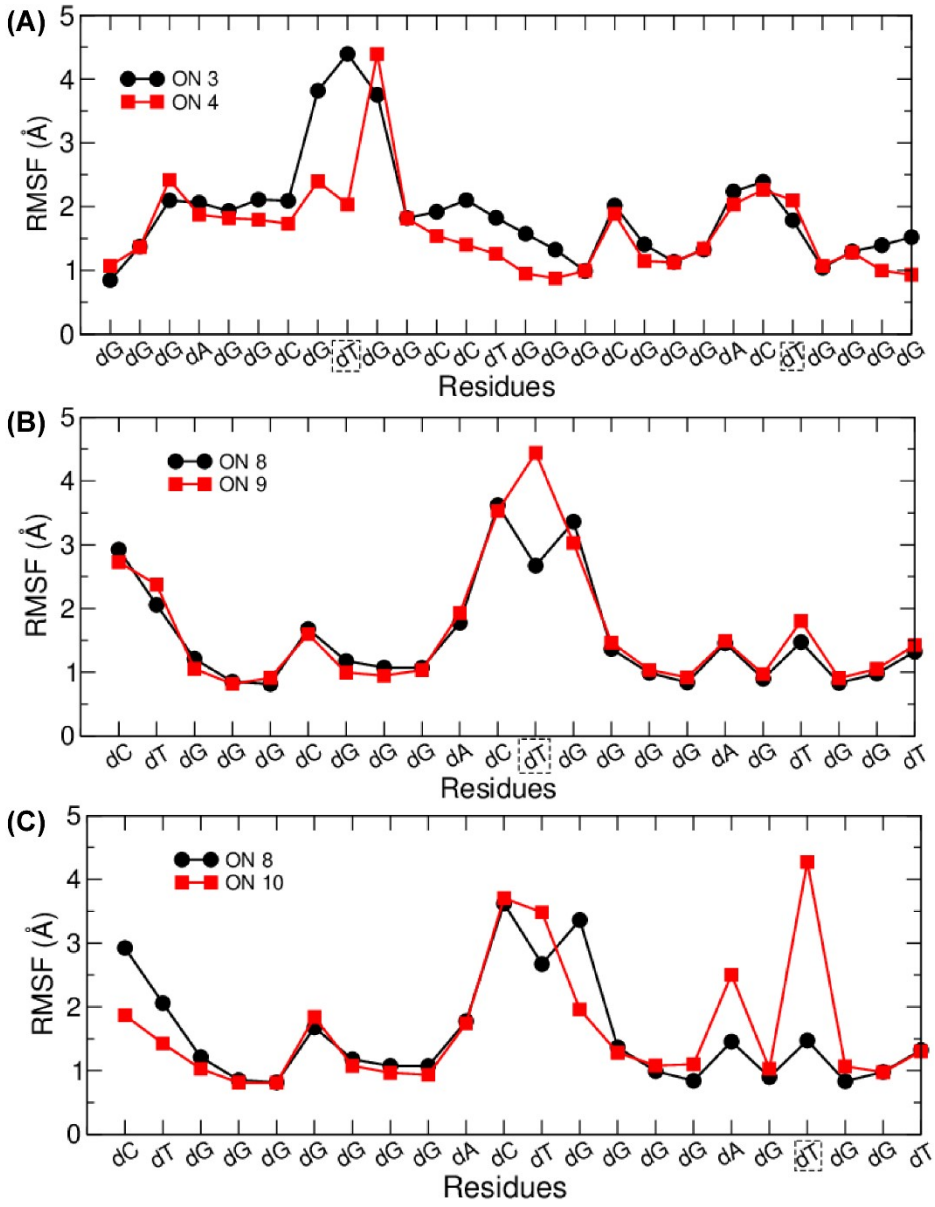

Fig. S17 RMSF plots of (**A**) LTR-III ON **3** and ON **4** with variation in the G_8 and FdU (**B**) LTR-IV ON **8** and ON **9** (**C**) LTR-IV ON **8** and ON **10** with variation in the probe. The nucleotides are represented from 5′ to 3′. The position of the probe has been indicated by a dashed box around the nucleotide RMSF values were calculated from the 500 ns MD simulations.

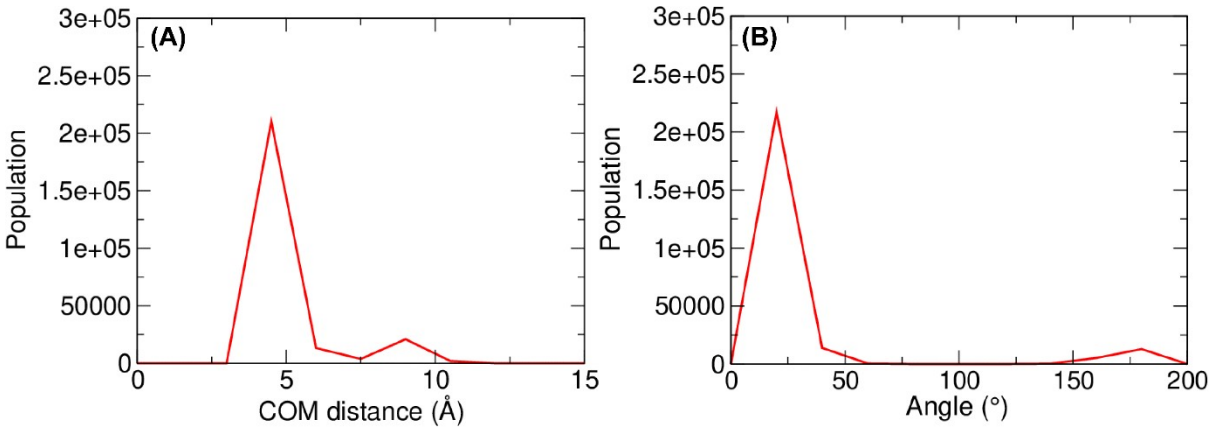

Fig. S18 Population distribution of the (**A**) centre of mass distance (COM) distance between G_{28} and FBFdU in ON **4**, (**B**) angle between the normal to G_{28} and FBFdU. The values were calculated from the 500 ns MD simulations.

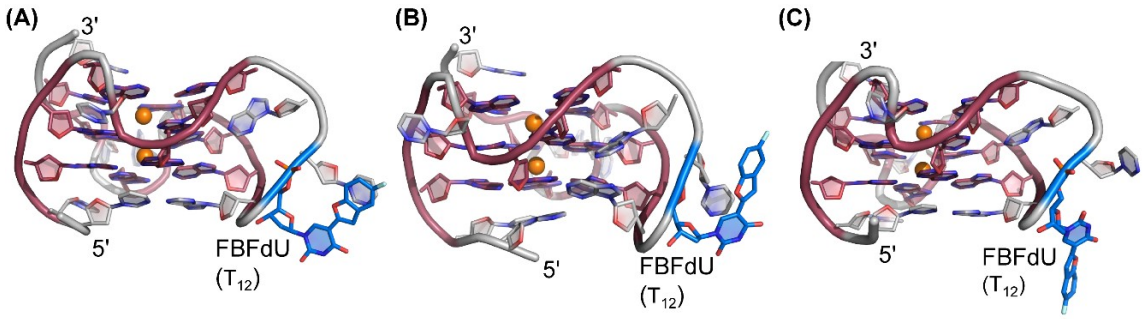

Fig. S19 Representative images of three major clusters of LTR-IV ON **9**. (**A**) Cluster 1, (**B**) cluster 2 and (**C**) cluster 3. GQ bases are represented in maroon and FBFdU in blue. K^+ ions are represented as orange spheres. Clusters have been obtained from the 500 ns MD simulation.
Model for ON **9** is available with the private link and access code (password): https://www.modelarchive.org/doi/10.5452/ma-6pmie Code: DG4iRTmwIz

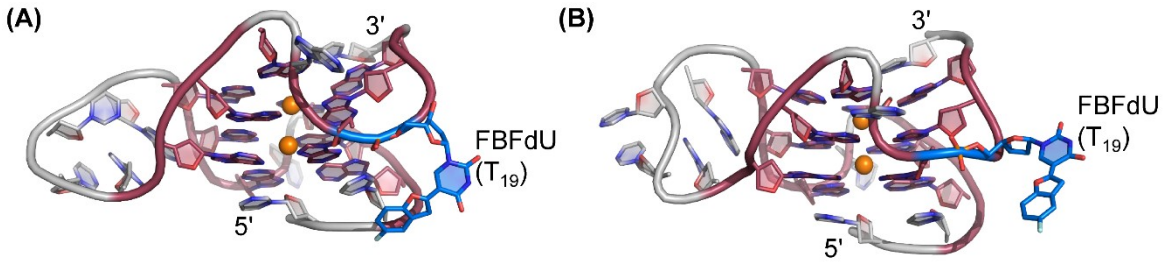

Fig. S20 Representative images of two major clusters of LTR-IV ON **10**. (**A**) Cluster 1 and (**B**) cluster 2. GQ bases are represented in maroon and FBFdU in blue. K^+ ions are represented as orange spheres. Clusters have been obtained from the 500 ns MD simulation. Model for ON **10** is available with the private link and access code (password): https://www.modelarchive.org/doi/10.5452/ma-otuxm
Code: INRqkxQXSJ

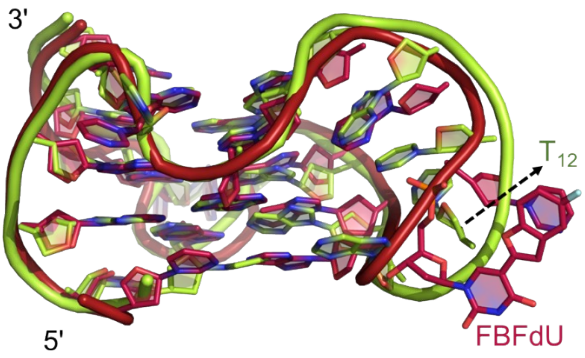

Fig. S21 Superimposed images of the major clusters of LTR-IV native ON **8** and modified ON **9**. ON **8** and **9** are represented in green and maroon, respectively. The bases, which show maximum changes in the orientation are labeled in the Figure. The clusters have been obtained from the 500 ns MD simulation.

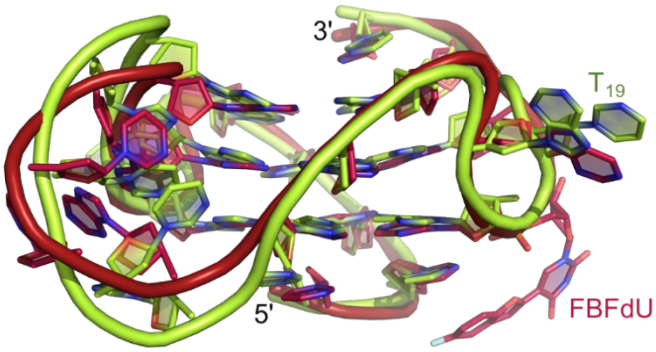

Fig. S22 Superimposed images of the major clusters of LTR-IV native ON **8** and modified ON **10**. ON **8** and **10** are represented in green and maroon, respectively. The bases, which show maximum changes in the orientation are labeled in the Figure. The clusters have been obtained from the 500 ns MD simulation.

11. Ligand binding studies of modified LTR ONs

Fluorescence: LTR GQ structures (0.5 μM) of ONs **4**, **9** and **16** were formed by heating the samples at 95 °C for 5 min in 20 mM potassium phosphate buffer (pH 7) containing 70 mM KCl. The samples were incubated with increasing concentrations of the ligands (TMPyP4 and BRACO19) at 25 °C for 1 h. Samples were excited at 330 nm with an excitation and emission wavelength slit widths of 7 nm and 9 nm, respectively. For DOX titration, increasing concentrations of annealed GQ formed by ON **12** in the same ionic conditions as mentioned above was incubated with DOX (2 μM) at 25 °C for 1 h. The final volume of each sample solution was kept at 200 μL. Samples were excited at 480 nm, with an excitation and emission slit widths of 7 nm and 9 nm respectively. Fluorescence experiments were performed in triplicate in a micro-fluorescence cuvette at 25 °C. For titration with TMPyP4 and BRACO19, an appropriate blank containing ligand in a buffer was subtracted from each reading for the corresponding ligand concentration. Normalized fluorescence intensity (F_N) against ligand concentration was plotted and fitted to a Hill equation (see below) to determine the apparent K_d values. Fitted graphs were prepared using OriginPro 8.5 software.[S19]

$$F_N = \frac{F_i - F_s}{F_0 - F_s}$$

F_i is the fluorescence intensity at each titration point. F_0 and F_s are the fluorescence intensity in the absence of ligand (L) and at saturation, respectively. n is the Hill coefficient or degree of cooperativity associated with the binding.

$$F_N = F_0 + (F_s - F_0)\left(\frac{[L]^n}{[K_d]^n + [L]^n}\right)$$

^{19}F NMR: LTR GQ structures of ONs **4** (45 μM), **9** (75 μM), **16** (45 μM) were formed by heating the samples at 95 °C for 5 min in 20 mM potassium phosphate buffer (pH 7) containing 70 mM KCl in 20% D_2O. The samples were allowed to cool at RT and then they were transferred to a Shigemi tube (5 mm advance NMR micro-tube) for NMR analysis. ^{19}F NMR spectra were recorded at a frequency 564.9 MHz on a Bruker AVANCE III HD ASCEND 600 MHz spectrometer equipped with Cryo-Probe (CP2.1 QCl 600S3 H/F-C/N-D-05 Z XT). After each experiment, increasing concentrations of ligands were added and incubated at RT for 1 h prior to the experiment. All ^{19}F NMR spectra were referenced relative to an external standard, trifluorotoluene (TFT = −63.72 ppm). Spectral parameters for ^{19}F NMR are same as mentioned in section 8. ^{19}F NMR spectra were obtained in 2–2.5 h with 5000–6000 scans. Spectra were processed with an exponential window function using lb = 20 Hz.

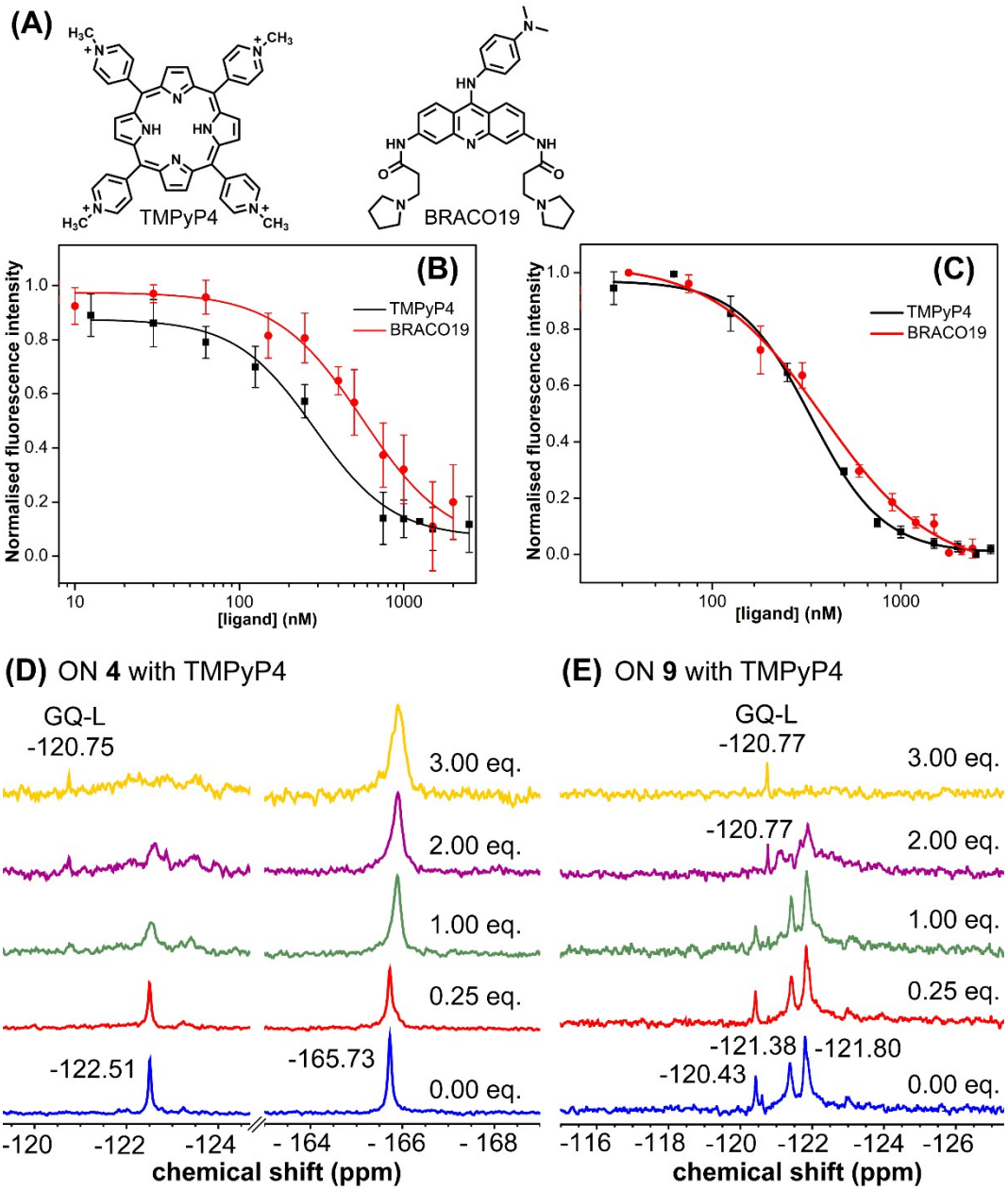

Fig. S23 (**A**) Chemical structures of GQ-binding ligands. Curve fits for the binding of TMPyP4 and BRACO19 to (**B**) LTR-III ON **4** and (**C**) LTR-IV ON **9**. Normalized fluorescence intensity at the emission maximum is plotted against ligand concentration. Values are denoted as mean ± s.d for 3 independent experiments. (**D** and **E**) ^{19}F NMR spectra of ONs **4** and **9** as a function of increasing TMPyP4 concentration. GQ-L represents peak corresponding to GQ-ligand complex.

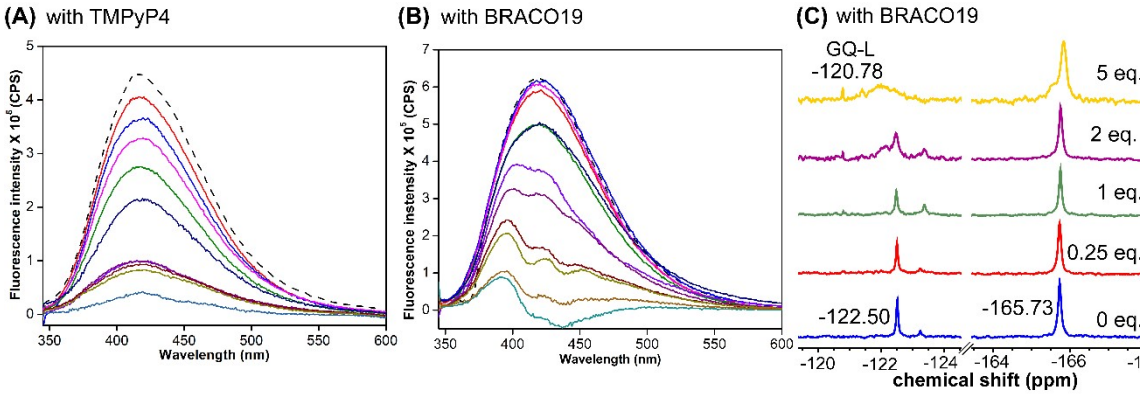

Fig. S24 Emission spectra for the titration of labeled LTR-III ON **4** (0.5 µM) with increasing concentration of (**A**) TMPyP4 (12.5 nM–2.5 µM) and (**B**) BRACO19 (10 nM–2.5 µM). Samples were excited at 330 nm with an excitation and emission slit widths of 7 nm and 9 nm, respectively. The dashed line represents the spectrum of ON **4** without any ligand. (**C**) ^{19}F NMR spectra of ON **4** (45 µM) with increasing BRACO19 concentration. GQ-L represents peak corresponding to GQ-ligand complex. See Section 11 for experimental details.

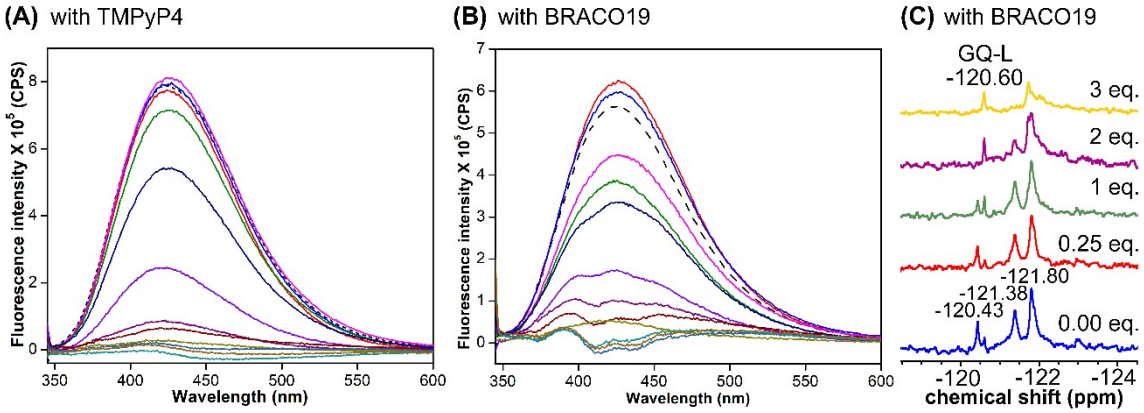

Fig. S25 Emission spectra for the titration of labeled LTR-IV ON **9** (0.5 µM) with increasing concentrations of (**A**) TMPyP4 (12.5 nM–2.5 µM) and (**B**) BRACO19 (36 nM–2.8 µM). Samples were excited at 330 nm with an excitation and emission slit widths of 7 nm and 9 nm, respectively. The dashed line represents the spectrum of ON **9** without any ligand. (**C**) ^{19}F NMR spectra of ON **9** (75 µM) with increasing BRACO19 concentration. GQ-L represents peak corresponding to GQ-ligand complex. See Section 11 for experimental details.

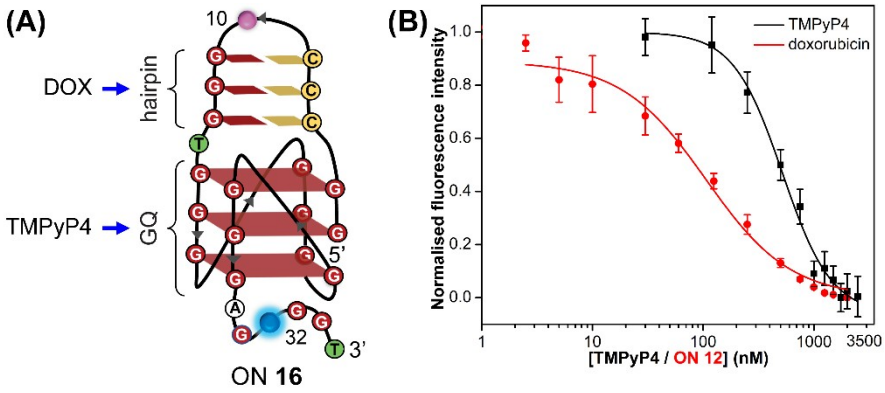

Fig. S26 FBFdU and FdU report structure-specific ligand binding to LTR GQ-hairpin structure. (**A**) Schematic representation of the doubly-labeled LTR ON **16** showing the preferred site of ligand (TMPyP4 to GQ and DOX to hairpin) interaction. (**B**) Curve fits for the binding of TMPyP4 and DOX to ON **16** (λ_{em}= 421 nm) and ON **12** (λ_{em}= 590 nm). Normalized fluorescence intensity at the emission maximum is plotted against ligand concentration. Values are denoted as mean ± s.d for 3 independent experiments. See Section 11 for experimental details.

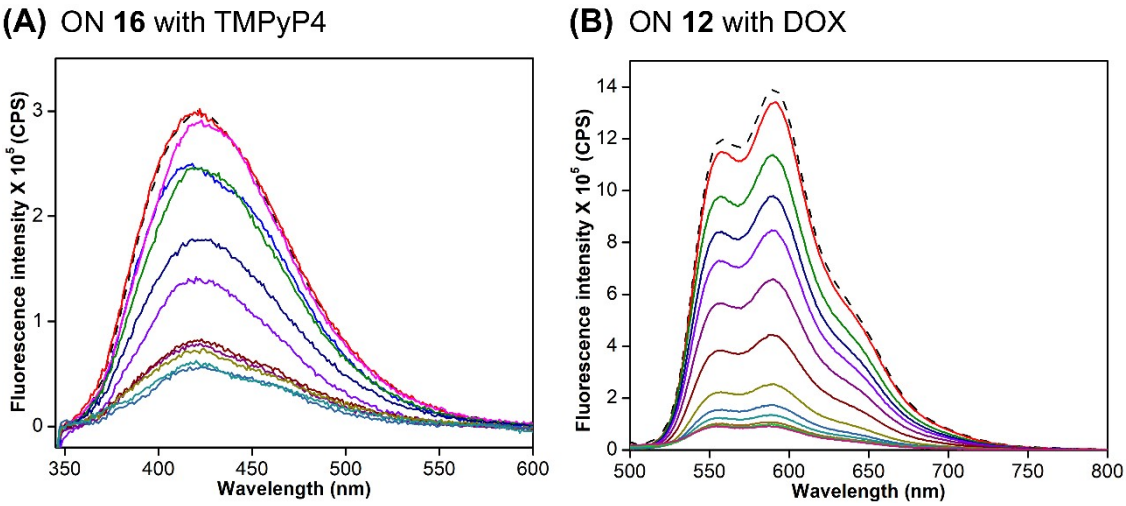

Fig. S27 (**A**) Emission spectra for the ligand titration of labeled LTR-(III+IV) ON **16** (0.5 µM) with increasing concentration of TMPyP4 (30 nM–2.5 µM). Samples were excited at 330 nm with an excitation and emission slit widths of 7 nm and 9 nm, respectively. The dashed line represents the spectrum of ON **16** without any ligand. (**B**) Emission spectra for the titration of DOX (2 µM) with increasing concentration of control ON **12** (2.5 nM–2.0 µM). Samples were excited at 480 nm with an excitation and emission slit widths of 7 nm and 9 nm, respectively. The dashed line represents the spectrum of DOX without any ON **12**.

12. *Taq* polymerase assay: 5′-FAM labeled primer **P1** (5 µM) and template DNA ONs **T1** and **T2** (5 µM) were annealed in 10 mM Tris-HCl (pH 7.8) containing 100 mM KCl at 95 °C for 5 minutes and slowly cooled to RT (Table S5). The primer-template duplexes were further diluted to 1 µM in 10 mM Tris-HCl buffer containing 100 mM KCl. Primer extension reactions were performed with primer-template duplex (100 nM), KCl (100 mM), 1× DNA polymerase buffer (10 mM Tris-HCl, pH 8.3, 50 mM KCl, 1.5 mM $MgCl_2$) at 37 °C. Reactions were initiated by adding dNTPs (500 µM) and 0.5 µL of *Taq* DNA polymerase (5 U/µL, New England Biolabs, Catlog. M0273S) in a total reaction volume of 20 µL. Reactions were stopped at different time intervals by adding 10 µL of denaturing

loading buffer (8.3 M urea in 10 mM Tris-HCl, 100 mM EDTA, 0.05% bromophenol blue, pH 8) further flash cooled on a dry-ice bath. The reaction mixture was then concentrated in a speedvac concentrator. The extension products were resolved by 15% denaturing PAGE containing 8.3 M urea and was electrophoresed at a constant power of 35 W for 2.5–3 h. The gel was scanned using an Amersham Typhon 600 (GE Healthcare) at the FAM wavelength and quantified with the help of the ImageJ software. Impact of ligands on the polymerase activity was studied by adding different concentrations of TMPyP4 and or DOX. The ligands were first added to the reaction mixture and incubated for 1 h at RT and then initiated by adding dNTPs and enzyme as above. The reaction products were analyzed as described above.

Table S5. Sequence of templates and primer used in *Taq* DNA polymerase stop assay.

ON	5′----------3′
P1	FAM-GGCAAAAAGCAGCTGCTTATATGCAG
T1	TTTTTGGGAGGCGTGGCCTGGGCGGGACTGGGGAGTGGTTTTTCTGCATATAAGCAGCTGCTTTTTGCC
T2[a]	TTTTTGGGAGGCGTGGCCTG**T**GCG**T**GACTGGGGAGTGGTTTTTCTGCATATAAGCAGCTGCTTTTTGCC

[a]**T** represents G-T mutation. This mutation does not support GQ formation.[S20]

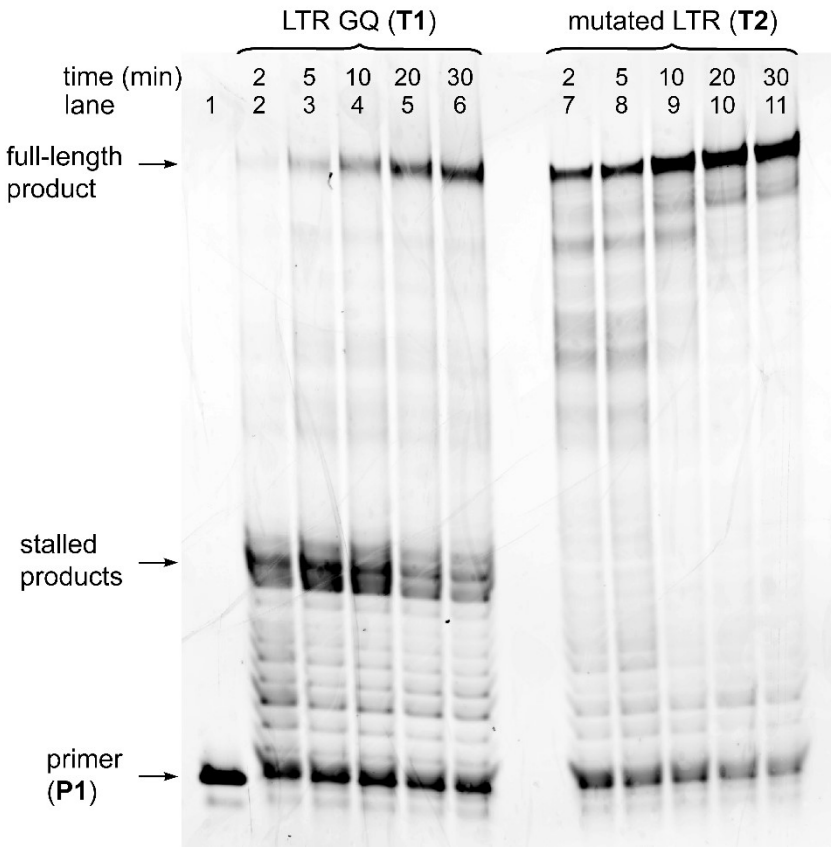

Fig. S28 Gel image of primer extension reactions using native LTR G-rich ON template **T1** and mutated LTR template **T2**. See Section 12 for details.

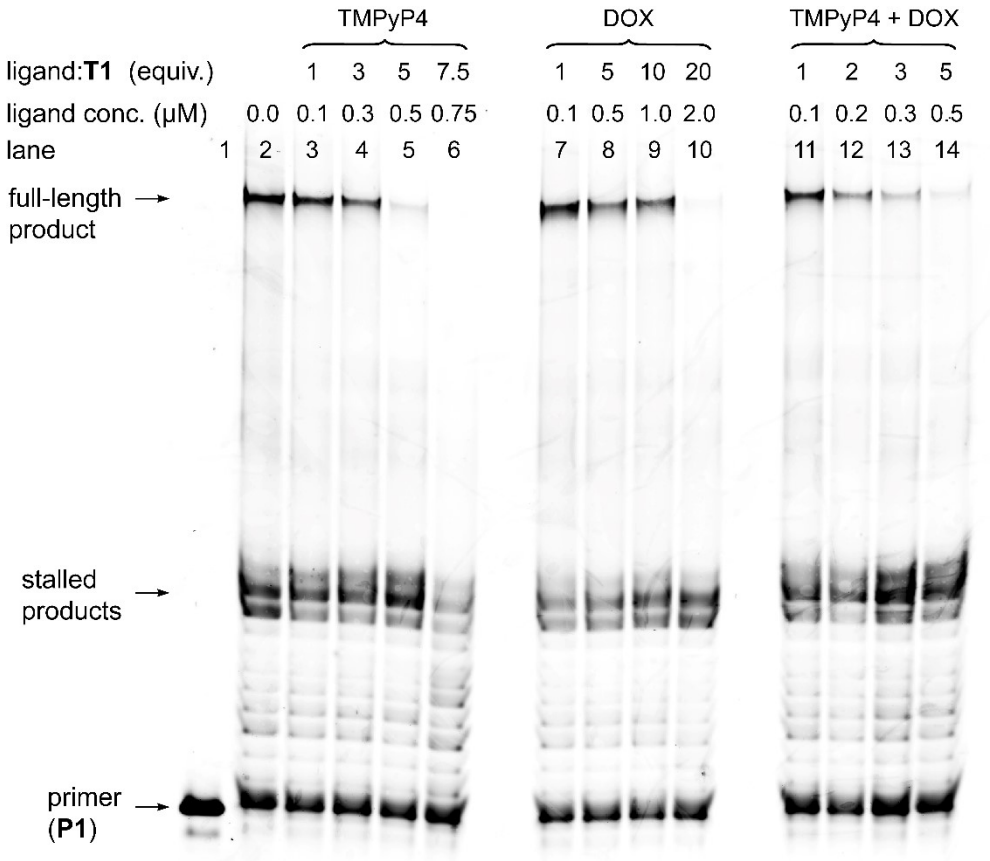

Fig. S29 Gel image of primer extension reactions using native LTR G-rich ON template **T1** in the presence of different ligands namely, TMPyP4/DOX and TMPyP4+DOX. See Section 12 for details.

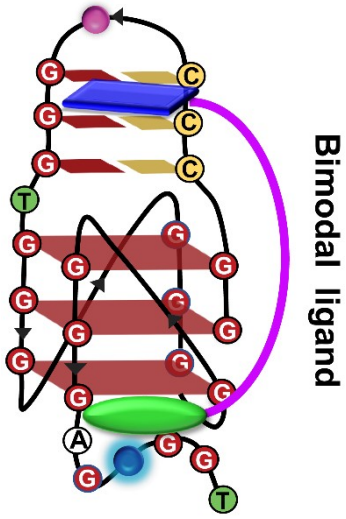

Fig. S30 Tailor-made bimodal ligand scaffolds composed of GQ and duplex binders could selectively interact with respective domains of LTR G-rich motif. The design of clamping linker (length and interaction partners) will be crucial in adding to the selectivity and location of binding within the GQ, hairpin and GQ-hairpin junction domains. Here, a representative mode of binding of the ligand scaffold is shown.

13. ^{31}P NMR of modified phosphoramidites

^{31}P NMR of **1a** (162 MHz, $CDCl_3$)

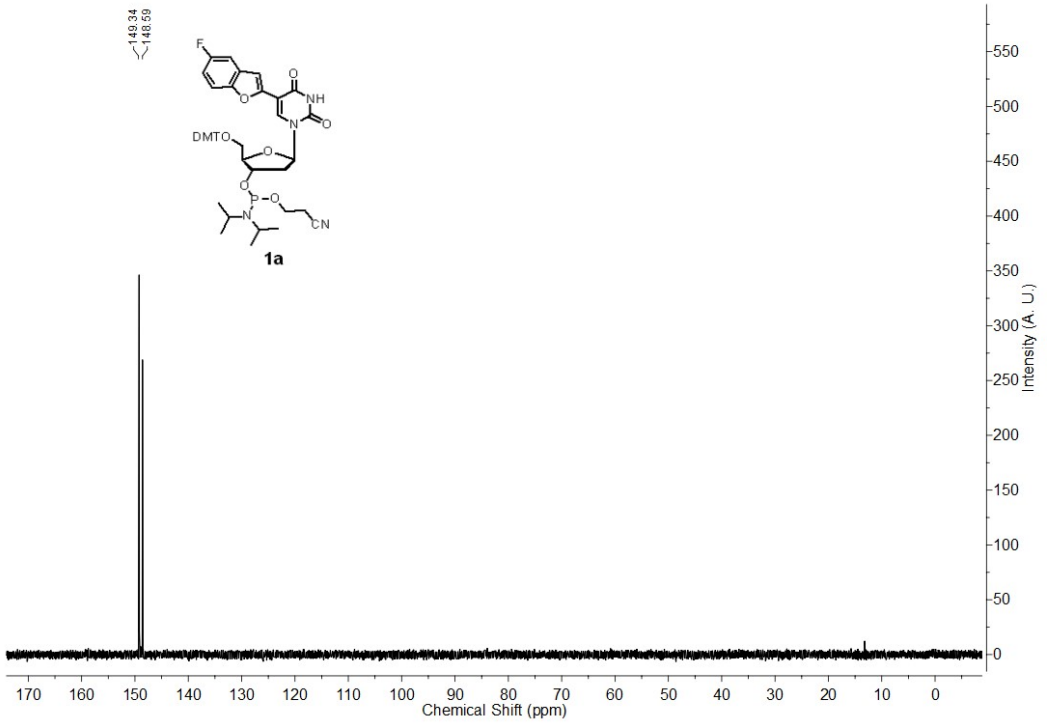

^{31}P NMR of **2a** (162 MHz, $CDCl_3$)

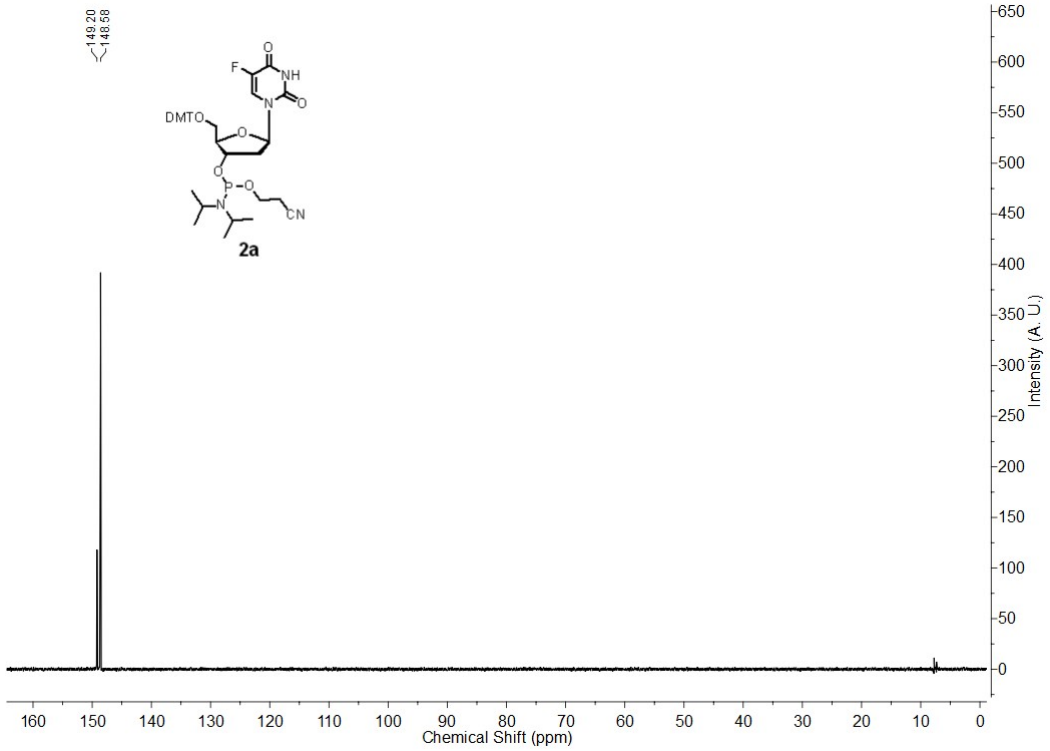

14. References

[S1] S. Manna, D. Sarkar, S. G. Srivatsan, *J. Am. Chem. Soc.* **2018**, *140*, 12622–12633.

[S2] L. Sacre, C. J. Wilds, *Eur. J. Org. Chem.* **2017**, 3003–3008.

[S3] A. Pandey, S. Roy, S. G. Srivatsan, *Chem. Asian J.* **2023**, *18*, e20230051.

[S4] P. Selenko, Z. Serber, B. Gadea, J. Ruderman, G. Wagner, *Proc. Natl. Acad. Sci. U. S. A.* **2006**, *103*, 11904–11909,

[S5] N. Yagi, K. Satonaka, M. Horio, H. Shimogaki, Y. Tokuda, S. Maeda, *Biotech Histochem*. **1996**, *71*, 123–129.

[S6] E. Butovskaya, B. Heddi, B. Bakalar, S. N. Richter, A. T. Phan, *J. Am. Chem. Soc.* **2018**, *140*, 13654–3662.

[S7] B. De Nicola, C. J. Lech, B. Heddi, S. Regmi, I. Frasson, R. Perrone, S. N. Richter, A.T. Phan, *Nucleic Acids Res.* **2016**, *44*, 6442–6451.

[S8] Gaussian 16, Revision B.01, M. J. Frisch, G. W. Trucks, H. B. Schlegel, G. E. Scuseria, M. A. Robb, J. R. Cheeseman, G. Scalmani, V. Barone, G. A. Petersson, H. Nakatsuji, X. Li, M. Caricato, A. V. Marenich, J. Bloino, B. G. Janesko, R. Gomperts, B. Mennucci, H. P. Hratchian, J. V. Ortiz, A. F. Izmaylov, J. L. Sonnenberg, D. Williams-Young, F. Ding, F. Lipparini, F. Egidi, J. Goings, B. Peng, A. Petrone, T. Henderson, D. Ranasinghe, V. G. Zakrzewski, J. Gao, N. Rega, G. Zheng, W. Liang, M. Hada, M. Ehara, K. Toyota, R. Fukuda, J. Hasegawa, M. Ishida, T. Nakajima, Y. Honda, O. Kitao, H. Nakai, T. Vreven, K. Throssell, J. A. Montgomery, Jr., J. E. Peralta, F. Ogliaro, M. J. Bearpark, J. J. Heyd, E. N. Brothers, K. N. Kudin, V. N. Staroverov, T. A. Keith, R. Kobayashi, J. Normand, K. Raghavachari, A. P. Rendell, J. C. Burant, S. S. Iyengar, J. Tomasi, M. Cossi, J. M. Millam, M. Klene, C. Adamo, R. Cammi, J. W. Ochterski, R. L. Martin, K. Morokuma, O. Farkas, J. B. Foresman, and D. J. Fox, Gaussian, Inc., Wallingford CT, 2016.

[S9] J. Wang, W. Wang, P. A. Kollman, D. A. Case, *J. Mol. Graph. Model.* **2006**, *25*, 247−260.

[S10] J. Wang, R. M. Wolf, J. W. Caldwell, P. A. Kollman, D. A. Case, *J. Comput. Chem.* **2004**, *25*, 1157−1174.

[S11] R. Galindo-Murillo, J. C. Robertson, M. Zgarbová, J. Šponer, M. Otyepka, P. Jurečka, T. E., Cheatham, III , *J. Chem. Theory Comput.* **2016**, *12*, 4114−4127.

[S12] S. Kumar, S. P. Pany, S. Sudhakar, S. B. Singh, C. S. Todankar, Pradeepkumar, P.I. *Biochemistry* **2022**, *61*, 2546−2549.

[S13] R. Salomon-Ferrer, A. W. Götz, D. Poole, S. Le Grand, R. C. Walker, *J. Chem. Theory Comput*. **2013**, *9*, 3878−3888.

[S14] A. W. Götz, M. J. Williamson, D. Xu, D. Poole, S. Le Grand, R. C. Walker, *J. Chem. Theory Comput.* **2012**, *8*, 1542−1555.

[S15] S. Le Grand, A. W. Götz, R. C. Walker, *Comput. Phys. Commun.* **2013**, *184*, 374−380.

[S16] D. A. Case, I. Y. Ben-Shalom, S. R. Brozell, D. S. Cerutti, T. E., Cheatham, III, V. W. D. Cruzeiro, T. A. Darden, R. E. Duke, D. Ghoreishi, M. K. Gilson, AMBER 2018; Univ. California: San Fr, **2018**; Vol. 2018.

[S17] D. R. Roe, T. E. Cheatham, *J. Chem. Theory Comput.* **2013**, *9*, 3084−3095.

[S18] W. Humphrey, A. Dalke, K. Schulten, *J. Molec. Graphics* **1996**, *14*, 33−38.

[S19] A. A. Tanpure, S. G. Srivatsan, *Nucleic Acids Res.* **2015**, *43,* e149.

[S20] M. Scalabrin, I. Frasson, E. Ruggiero, R. Perrone, E. Tosoni, S. Lago, M. Tassinari, G. Palù, S. N. Richter, *Sci. Rep.* **2017**, *7*, 45244.